

From Astrophysicist to Data Scientist in Three Acts: navigating an academic career with a short attention span

Jill P. Naiman
Teaching Assistant Professor, iSchool
astronaiman.com

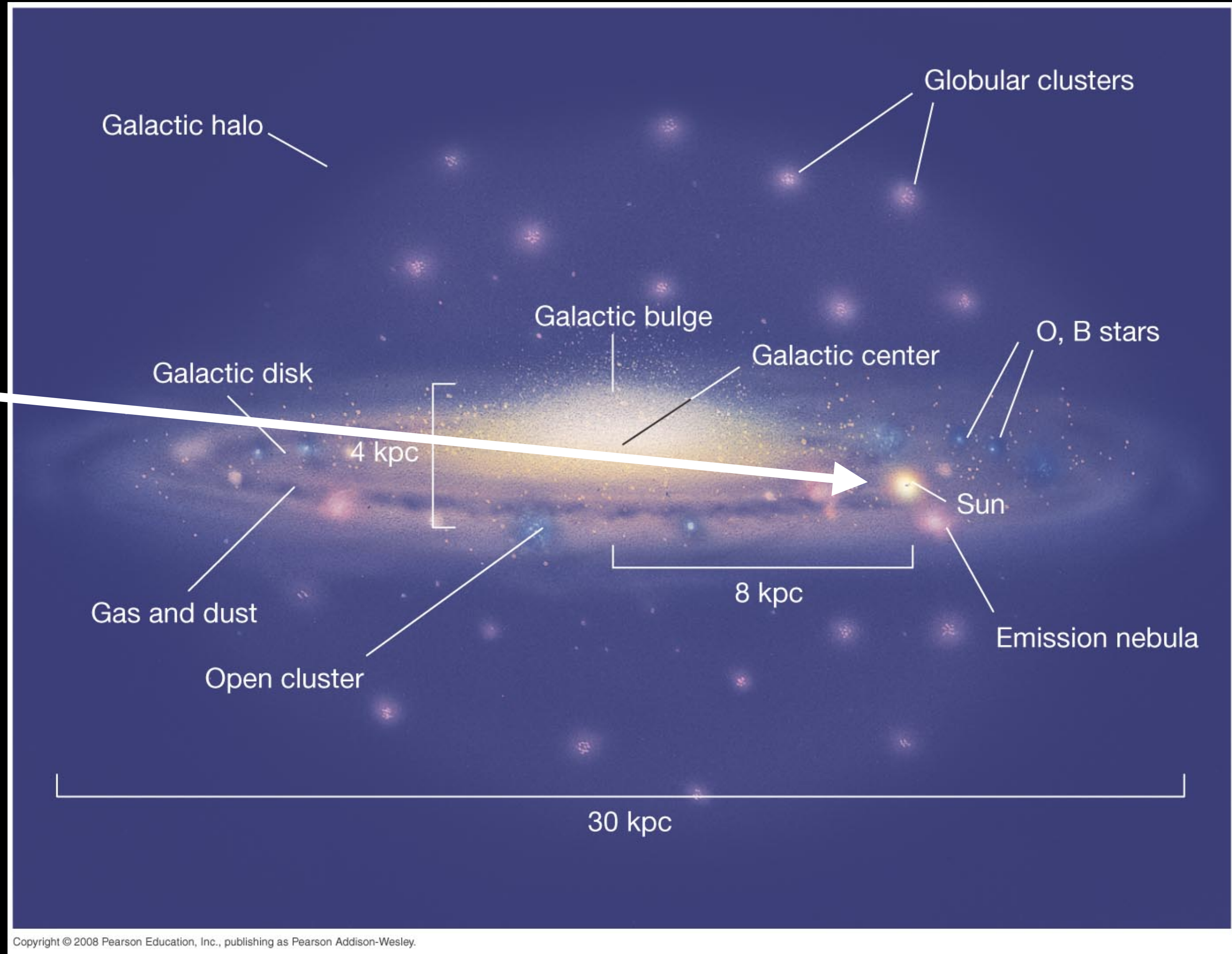
Act I: Astronomy & Astrophysics

Act II: Data Visualization

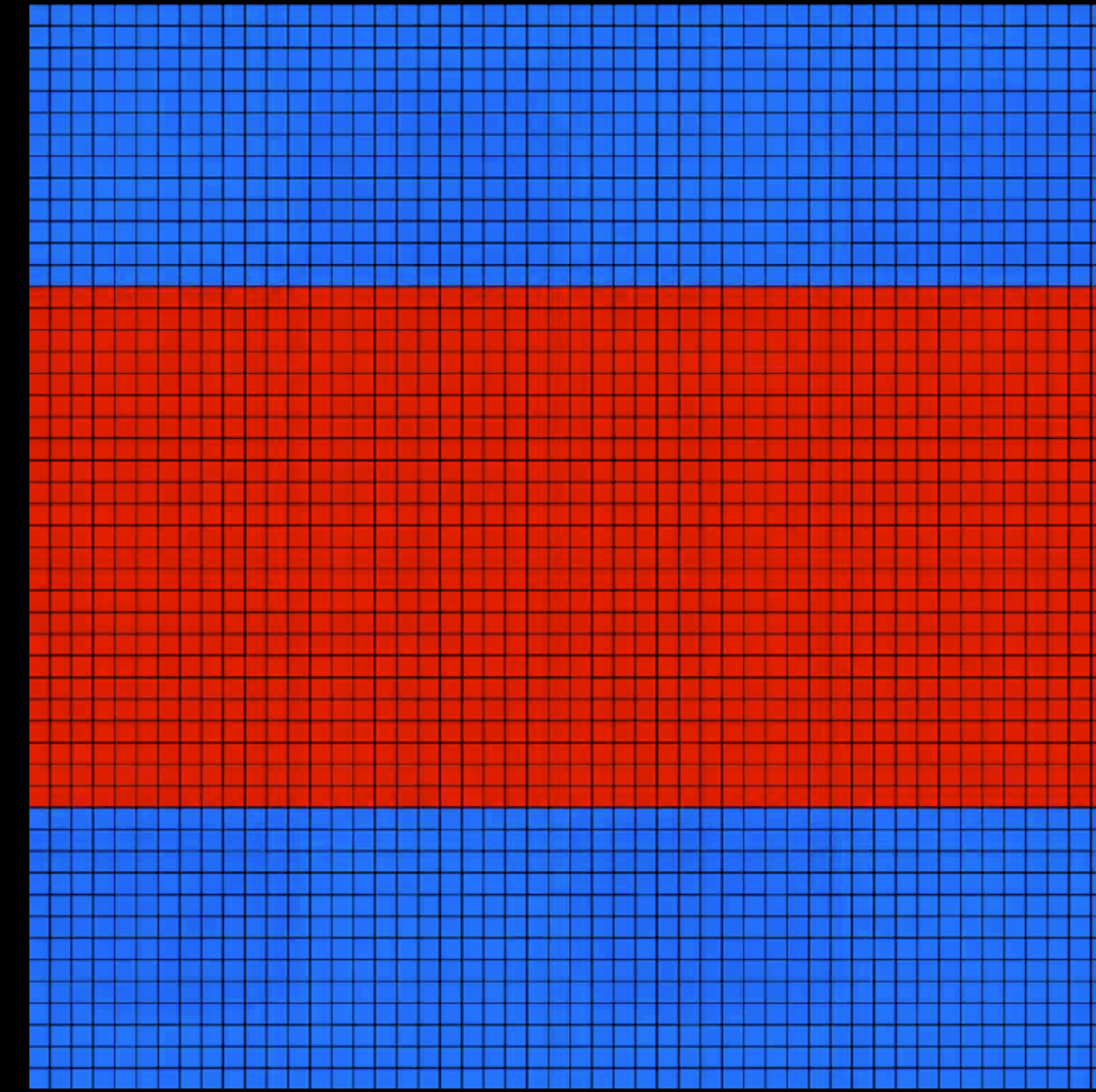
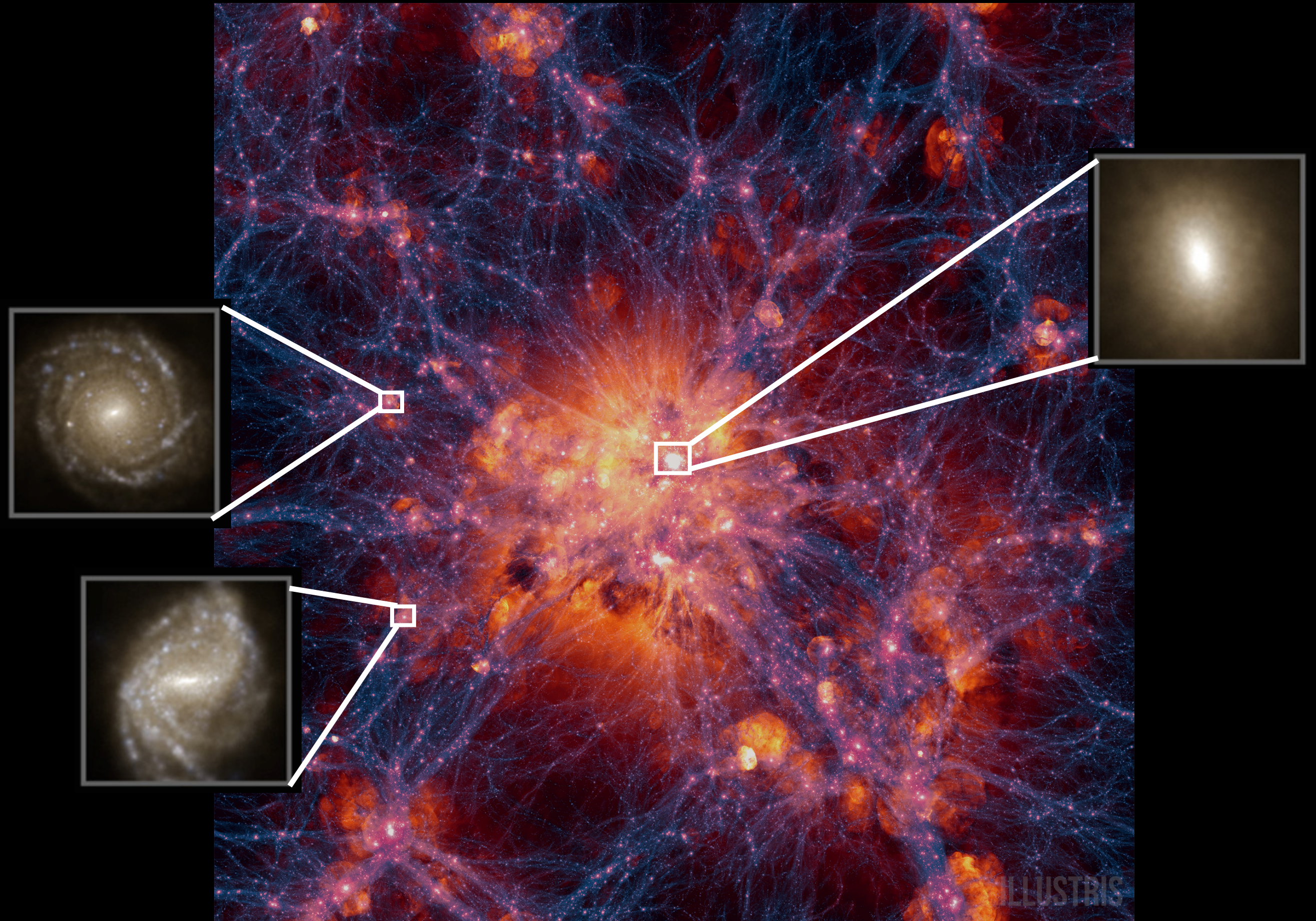
Act III: Information Scientist?

Act I: Astronomy & Astrophysics

Earth is ~ here



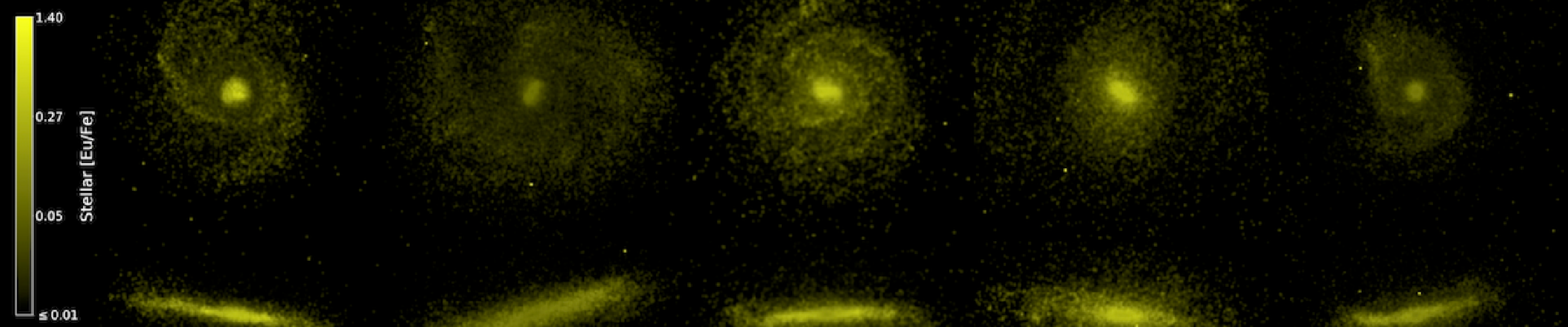
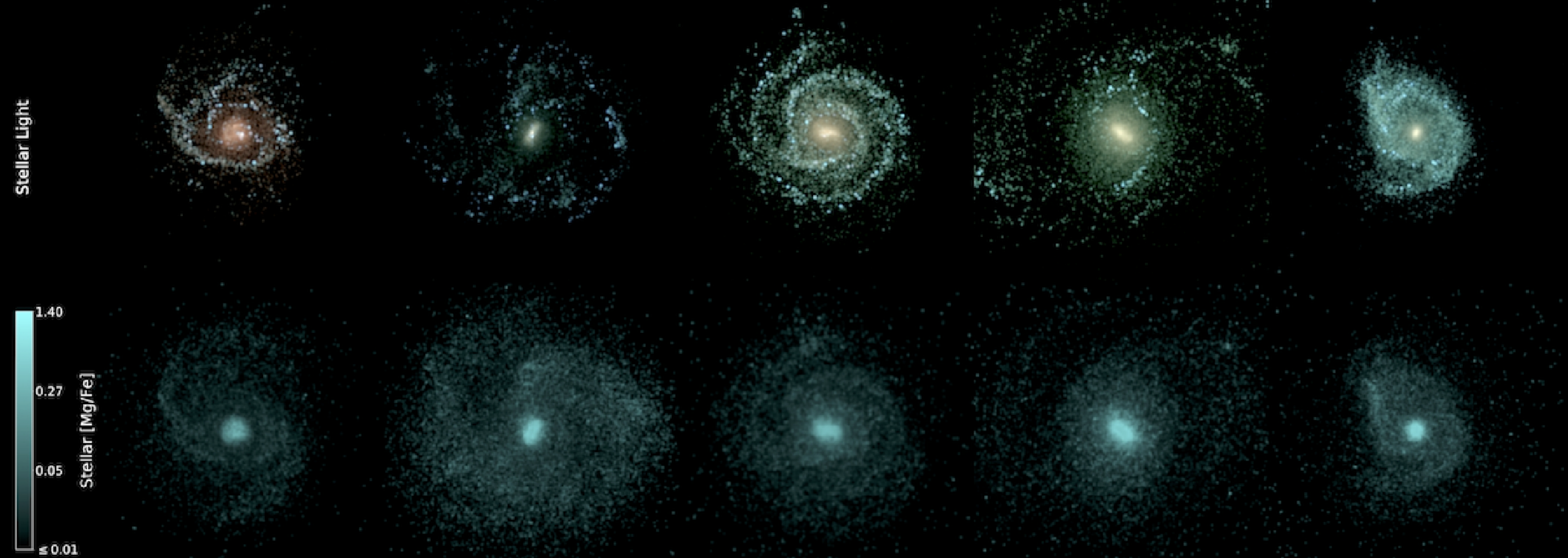
IllustrisTNG Simulations



Moving mesh (AREPO)

Simulating Cosmological Galaxy Formation: A Problem of Scales

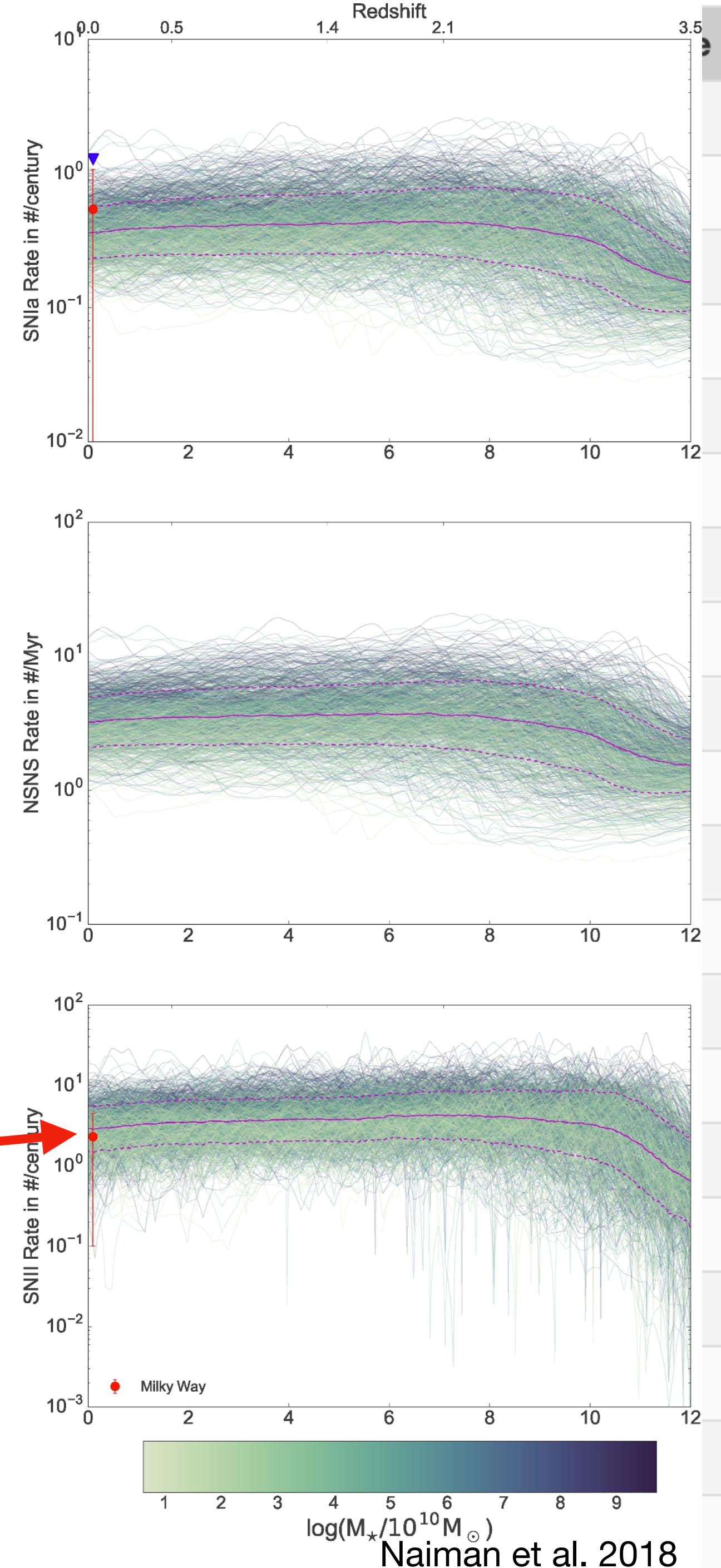
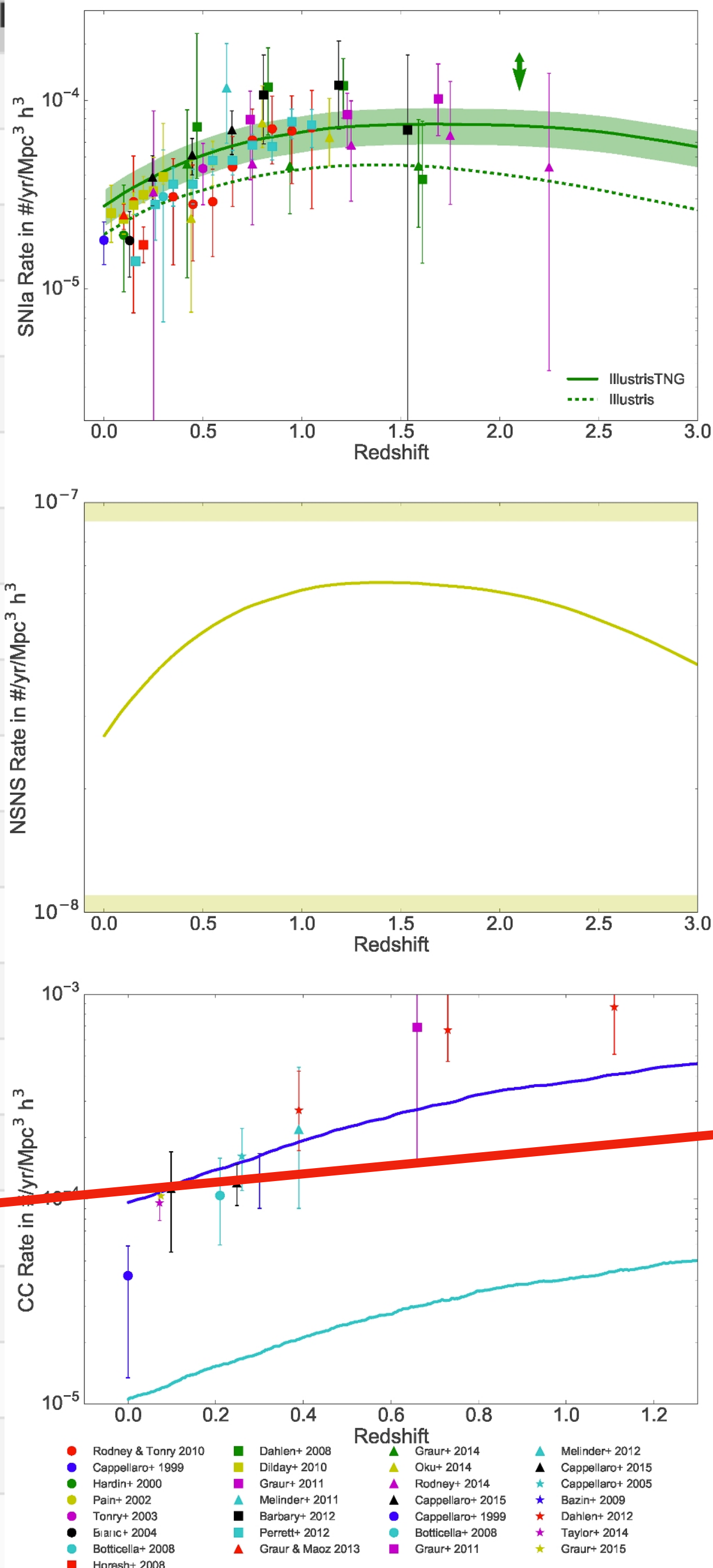
1 Mpc $\sim 3.1 \times 10^{22}$ meters



Run	Alt. Name	Total NumPart (DM)	Chunks per Snapshot	Full Snapshot Size	Avg Groupcat Size	Total Data Volume
L35n270TNG	TNG50-4	19,683,000	11	5.2 GB	20 MB	0.6 TB
L35n270TNG_DM	TNG50-4-Dark	19,683,000	4	1.2 GB	10 MB	0.1 TB
L35n540TNG	TNG50-3	157,464,000	11	44 GB	130 MB	7.5 TB
L35n540TNG_DM	TNG50-3-Dark	157,464,000	4	9.4 GB	50 MB	0.6 TB
L35n1080TNG	TNG50-2	1,259,712,000	128	350 GB	860 MB	18 TB
L35n1080TNG_DM	TNG50-2-Dark	1,259,712,000	85	76 GB	350 MB	4.5 TB
L35n2160TNG	TNG50-1	10,077,696,000	680	2.7 TB	7.2 GB	~320 TB
L35n2160TNG_DM	TNG50-1-Dark	10,077,696,000	128	600 GB	2.3 GB	36 TB
L75n455TNG	TNG100-3	94,196,375	7	27 GB	110 MB	1.5 TB
L75n455TNG_DM	TNG100-3-Dark	94,196,375	4	5.7 GB	40 MB	0.4 TB
L75n910TNG	TNG100-2	753,571,000	56	215 GB	650 MB	14 TB
L75n910TNG_DM	TNG100-2-Dark	753,571,000	8	45 GB	260 MB	2.8 TB
L75n1820TNG	TNG100-1	6,028,568,000	448	1.7 TB	4.3 GB	128 TB
L75n1820TNG_DM	TNG100-1-Dark	6,028,568,000	64	360 GB	1.7 GB	22 TB
L205n625TNG	TNG300-3	244,140,625	16	63 GB	340 MB	4 TB
L205n625TNG_DM	TNG300-3-Dark	244,140,625	4	15 GB	130 MB	1 TB
L205n1250TNG	TNG300-2	1,953,125,000	100	512 GB	2.2 GB	31 TB
L205n1250TNG_DM	TNG300-2-Dark	1,953,125,000	25	117 GB	810 MB	7.2 TB
L205n2500TNG	TNG300-1	15,625,000,000	600	4.1 TB	14 GB	235 TB
L205n2500TNG_DM	TNG300-1-Dark	15,625,000,000	75	930 GB	5.2 GB	57 TB

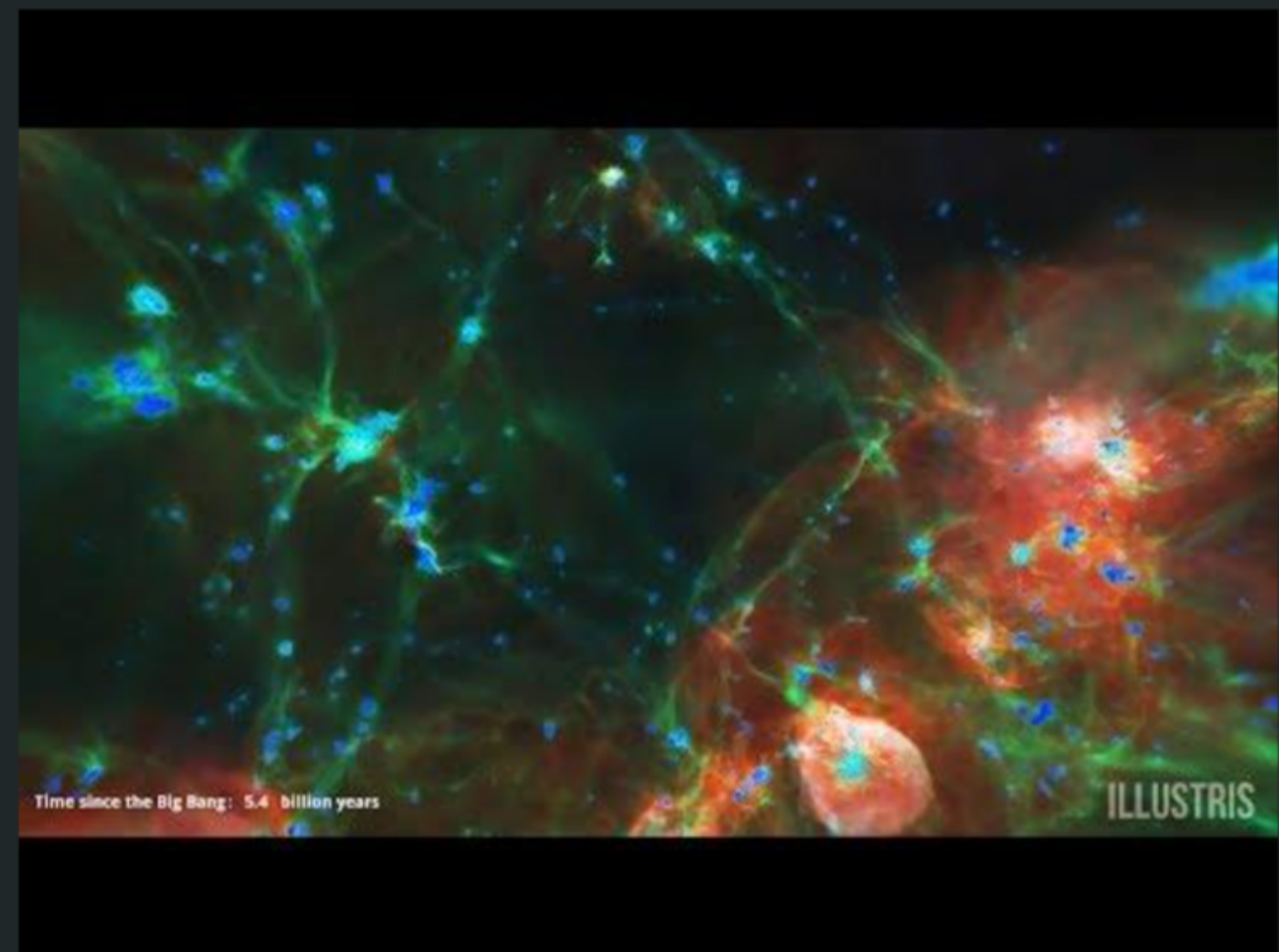
Run	Alt. Name	Total NumPart (DM)	Chunks per Snapshot	Full Snapshot Size	Avg Groupcat Size	Total Data Volume
L35n270TNG	TNG50-4	19,683,000	11	5.2 GB	20 MB	0.6 TB
L35n270TNG_DM	TNG50-4-Dark	19,683,000	4	1.2 GB	10 MB	0.1 TB
L35n540TNG	TNG50-3	157,464,000	11	44 GB	130 MB	7.5 TB
L35n540TNG_DM	TNG50-3-Dark	157,464,000	4	9.4 GB	50 MB	0.6 TB
L35n1080TNG	TNG50-2	1,259,712,000	128	350 GB	860 MB	18 TB
L35n1080TNG_DM	TNG50-2-Dark	1,259,712,000	85	76 GB	350 MB	4.5 TB
L35n2160TNG	TNG50-1	10,077,696,000	680	2.7 TB	7.2 GB	~320 TB
L35n2160TNG_DM	TNG50-1-Dark	10,077,696,000	128	600 GB	2.3 GB	36 TB
L75n455TNG	TNG100-3	94,196,375	7	27 GB	110 MB	1.5 TB
L75n455TNG_DM	TNG100-3-Dark	94,196,375	4	5.7 GB	40 MB	0.4 TB
L75n910TNG	TNG100-2	753,571,000	56	215 GB	650 MB	14 TB
L75n910TNG_DM	TNG100-2-Dark	753,571,000	8	45 GB	260 MB	2.8 TB
L75n1820TNG	TNG100-1	6,028,568,000	448	1.7 TB	4.3 GB	128 TB
L75n1820TNG_DM	TNG100-1-Dark	6,028,568,000	64	360 GB	1.7 GB	22 TB
L205n625TNG	TNG300-3	244,140,625	16	63 GB	340 MB	4 TB
L205n625TNG_DM	TNG300-3-Dark	244,140,625	4	15 GB	130 MB	1 TB
L205n1250TNG	TNG300-2	1,953,125,000	100	512 GB	2.2 GB	31 TB
L205n1250TNG_DM	TNG300-2-Dark	1,953,125,000	25	117 GB	810 MB	7.2 TB
L205n2500TNG	TNG300-1	15,625,000,000	600	4.1 TB	14 GB	235 TB
L205n2500TNG_DM	TNG300-1-Dark	15,625,000,000	75	930 GB	5.2 GB	57 TB

Run	Alt. Name	Total NumPart (DM)	Chu
L35n270TNG	TNG50-4	19,683,000	
L35n270TNG_DM	TNG50-4-Dark	19,683,000	
L35n540TNG	TNG50-3	157,464,000	
L35n540TNG_DM	TNG50-3-Dark	157,464,000	
L35n1080TNG	TNG50-2	1,259,712,000	
L35n1080TNG_DM	TNG50-2-Dark	1,259,712,000	
L35n2160TNG_DM	TNG50-1-Dark	10,077,696,000	
L75n455TNG	TNG100-3	94,196,375	
L75n455TNG_DM	TNG100-3-Dark	94,196,375	
L75n910TNG	TNG100-2	753,571,000	
L75n910TNG_DM	TNG100-2-Dark	753,571,000	
L75n1820TNG	TNG100-1	6,028,568,000	
L75n1820TNG_DM	TNG100-1-Dark	6,028,568,000	
L205n625TNG	TNG300-3	244,140,625	
L205n625TNG_DM	TNG300-3-Dark	244,140,625	
L205n1250TNG	TNG300-2	1,953,125,000	
L205n1250TNG_DM	TNG300-2-Dark	1,953,125,000	
L205n2500TNG	TNG300-1	15,625,000,000	
L205n2500TNG_DM	TNG300-1-Dark	15,625,000,000	

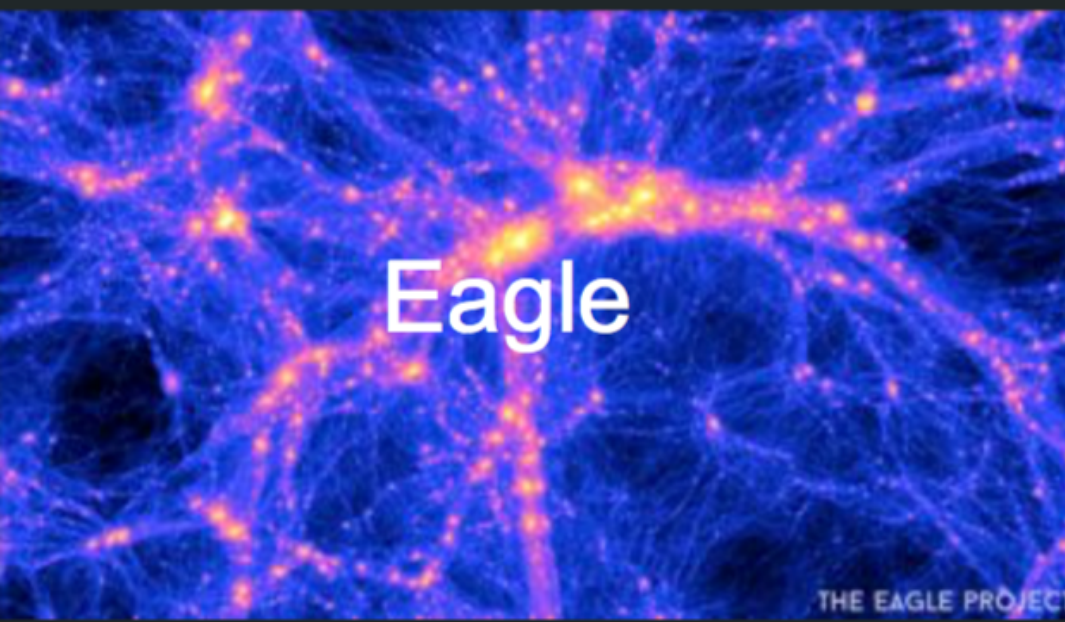


Act II: Data Visualization

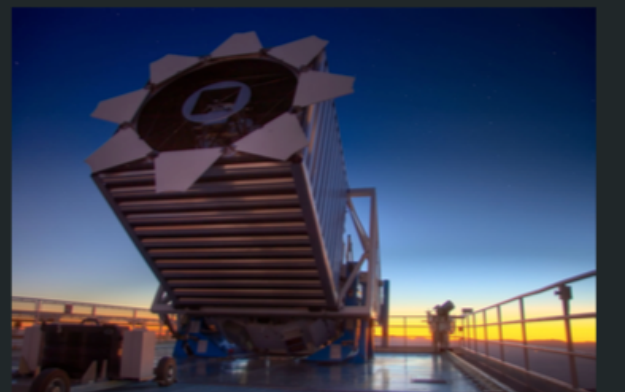
Scientists have lots of data



IllustrisTNG: Tens of TB



Scientists have lots of data



Sloan Digital Sky Survey: ~ 120TB (already)



Dark Energy Survey: ~200GB/night, ~PB last decade

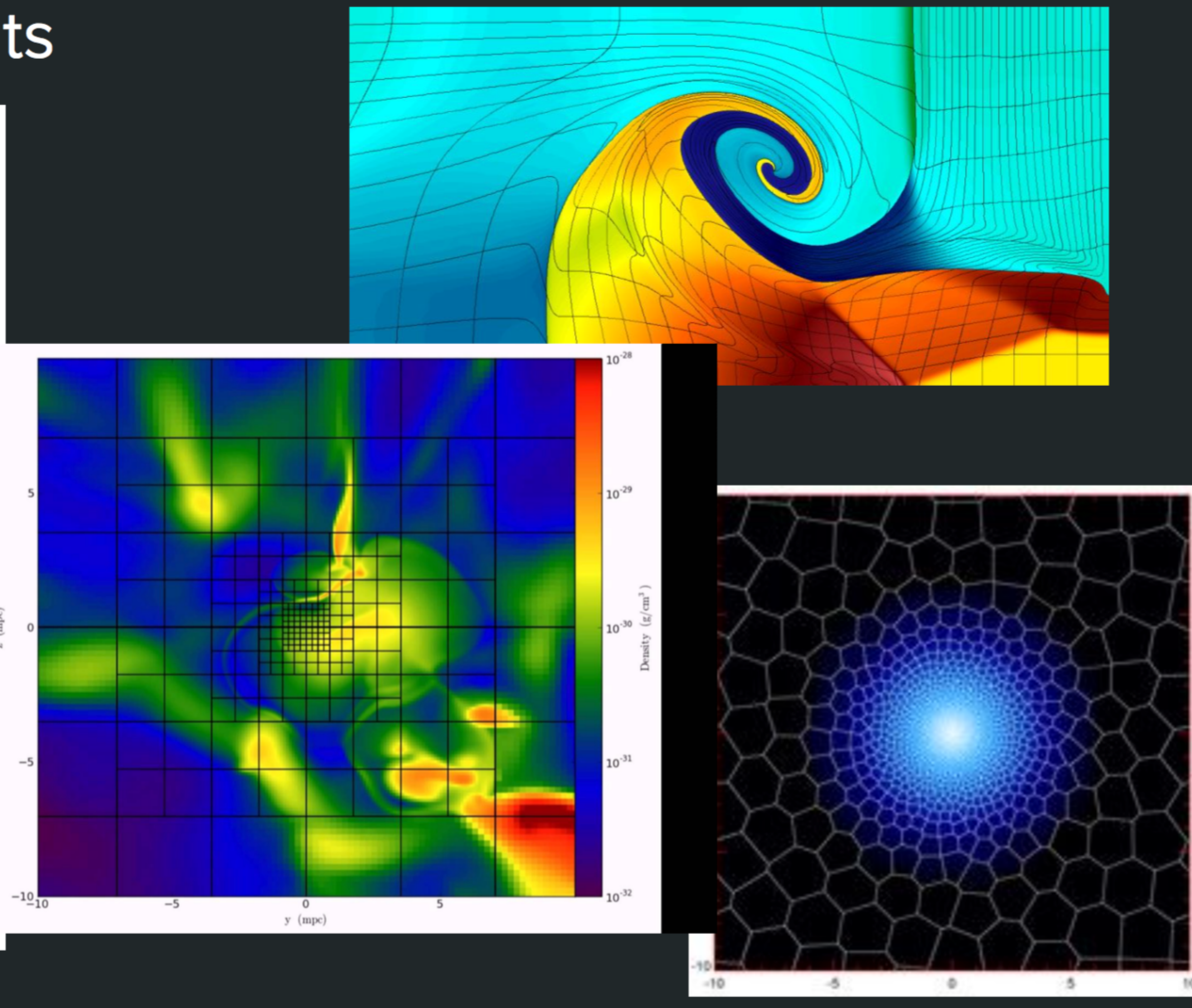
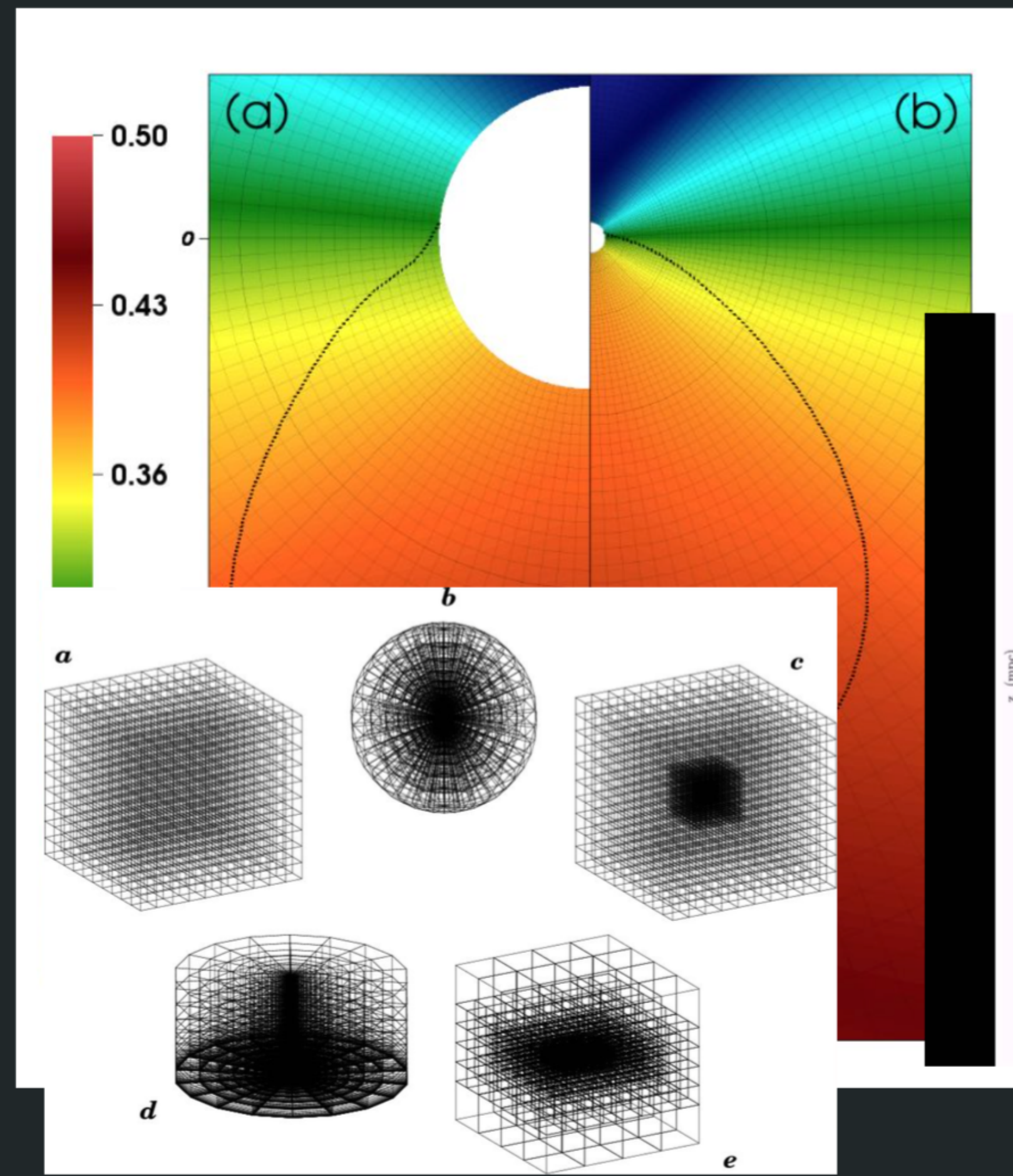


Large Synoptic Survey Telescope - 200PB/decade



Square Kilometre Array: 1000PB/year

The Data is in weird formats



Blender

- 3D modeling and animating program (free Maya)
- used by 3D graphics folks and a few astronomers
- Python API

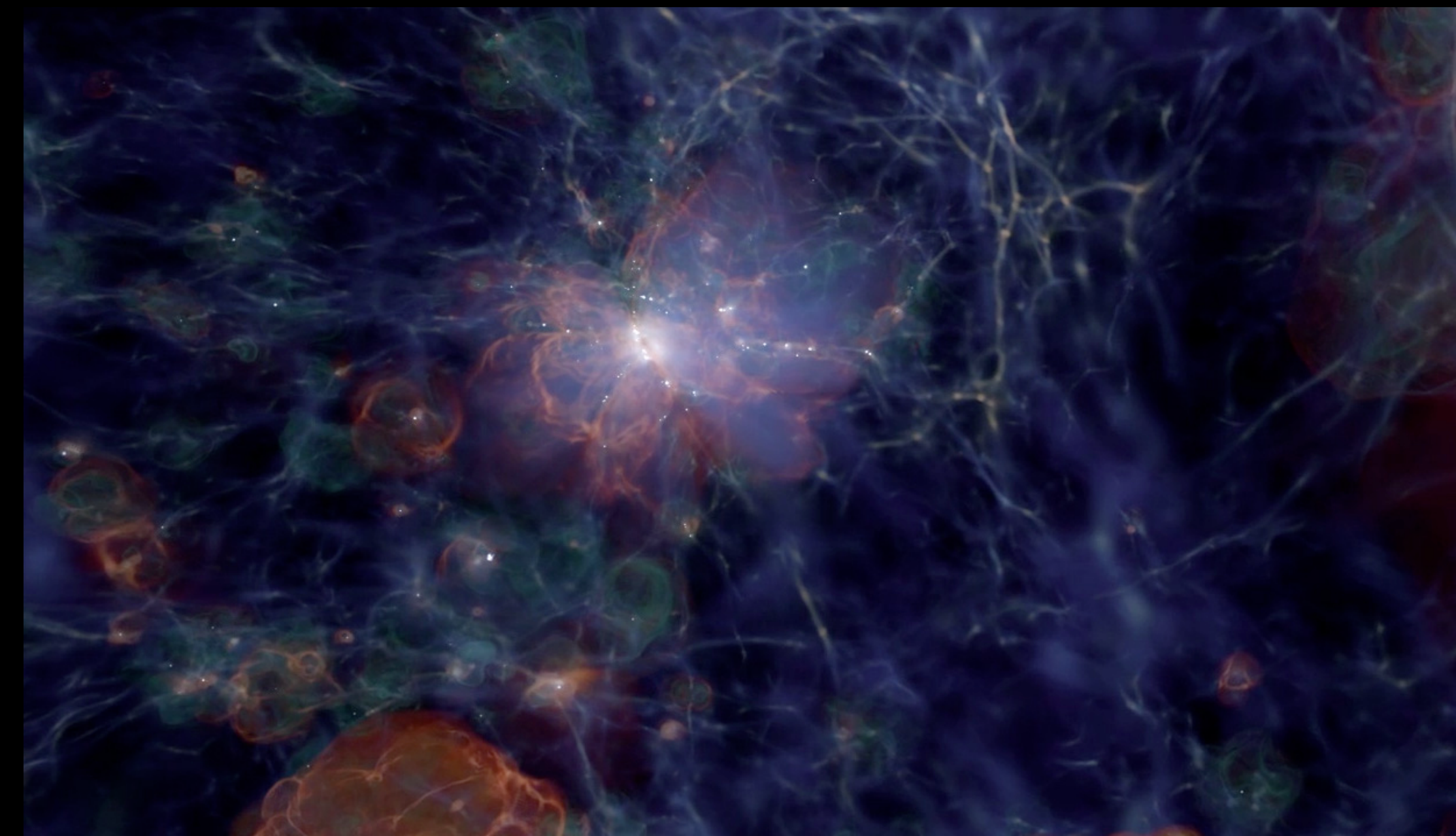


Gab 2012 <http://gablich.wordpress.com/>

Houdini™



Visualization with the Advanced Visualization Lab (NCSA)

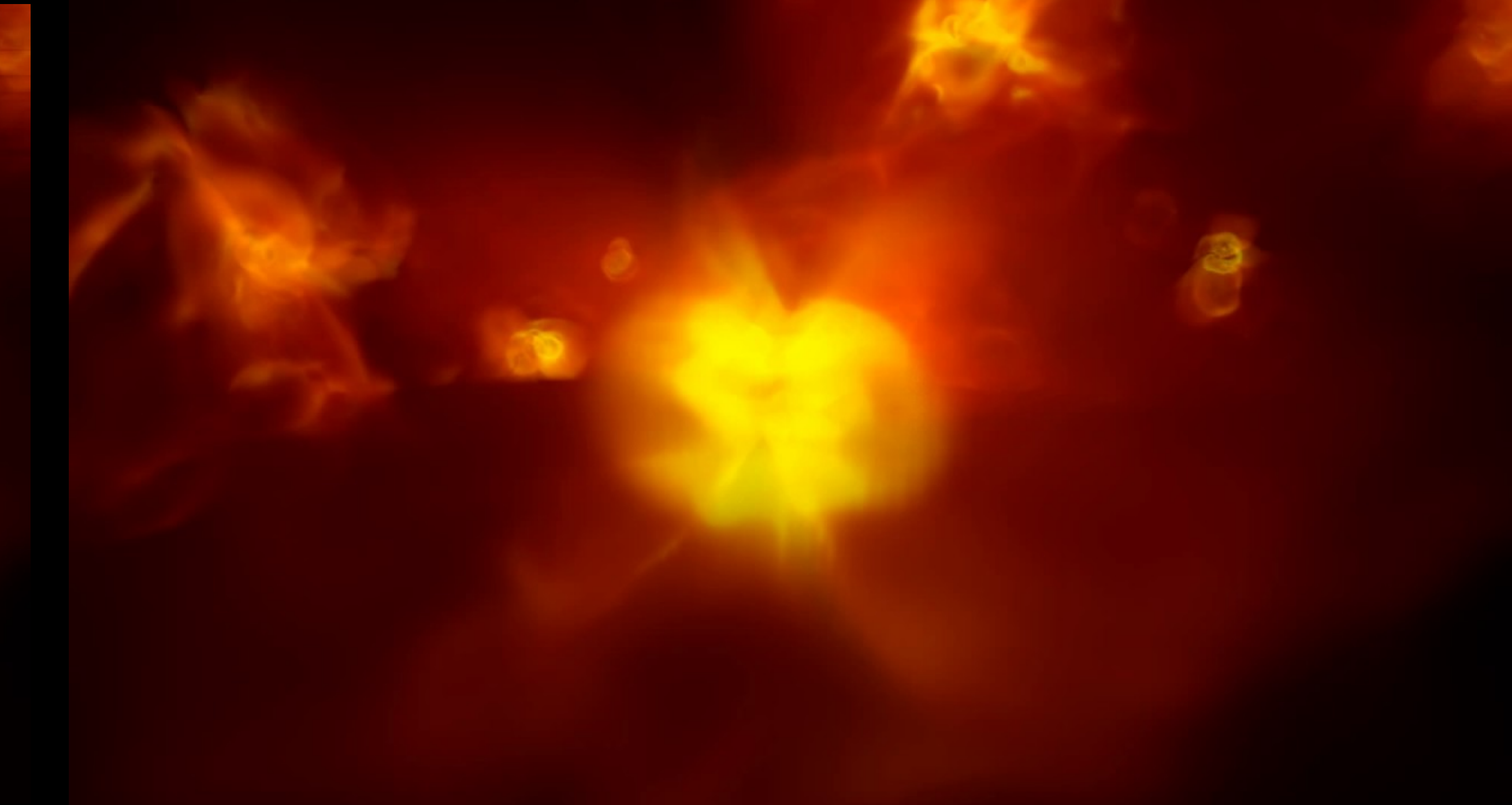


http://www.ncsa.illinois.edu/enabling/vis/cadens/documentation/beginning_of_time

ytini.com/blog.html



“Raw”



ytini



Scientific Visualization as an Educational Tool

Workshops/Short courses:

<https://www.astroblend.com/ba2016/>

<https://www.astroblend.com/ba2017/>

https://jnaiman.github.io/csci-p-14110_su2020/

https://jnaiman.github.io/csci-p-14110_su2019/

Scientific Visualization as an Educational Tool

Workshops/Short courses:

<https://www.astroblend.com/ba2016/>

<https://www.astroblend.com/ba2017/>

https://jnaiman.github.io/csci-p-14110_su2020/

https://jnaiman.github.io/csci-p-14110_su2019/

https://uiuc-ischool-dataviz.github.io/is445_spring2022/

Act III: Information Science?

(Digitization? Curriculum development? Visualization analytics? Science nomad?)

Impact Analysis with NLP on AVL Documentaries

Based on Rezapour & Diesner 2017

With iSchool students: Alistair Nunn, Anuska Gami, Shriya Srikanth
& in collaboration with the AVL

Positive shift in knowledge	“Very educational...learned a lot”
Negative shift in knowledge	“This is the biggest lie”
Positive interest in science topic	“My heart warms as we uncover the most unique and fascinating secrets of the universe”
Negative interest in science topic	“A waste of time and resources”
Positive engagement with film	“I like the piano”
Negative engagement with film	“Man this narrator gets pretty annoying after 7-10 min”
Impersonal report	“From the intro, none of this exists yet”
Personal opinion	“There will be a time when they all will be face to face with the creator of the universal”

The screenshot shows a YouTube video player. The video title is "Seeing the Beginning of Time 4k" by SpaceRip. It has 2,658,243 views and was uploaded on April 19, 2019. The video duration is 47:57. Below the video, there is a description encouraging viewers to check out their sister network MagellanTV. The comment section shows 1,852 comments. A comment from user 'b' reads: "Add a public comment...". Another comment from 'Robert F' says: "The vastness of space is so scary yet exciting to me for the amount of unknown possibilities that exist in it we are yet to know of or understand.". A third comment from 'Renegade5150' says: "Fantastic SpaceRip!! To everyone who was involved in the making of this brilliant video, from its deep and thought-provoking content, to its intricate and beautiful visuals, I say Bravo! I loved it."

Table from Anushka Gami (Oct 11th SPIN talk)

ILLINOIS
NCSA | National Center for
Supercomputing Applications
AVL | Advanced Visualization Lab



Kalina Borkiewicz



Jeff Carpenter



Stuart Levy



Eric Jensen
Brinson Civic Science Fellow
Assoc. Prof. University of Warwick, Sociology

ILLINOIS
School of Information Sciences



Jill Naiman

Digitizing Science: Indexing the Astronomical Literature

1840 A. R. MARSTON: RINGS AROUND WR STARS

Table Multiple ring nebulae observed.

	Observed	Filter	Exposure (secs)	Figure
WR10	May 1994	H α	1800	2
WR40	May 1994	H α	900	3a
WR40	19 May 1994	[OIII]	2100	3b
WR75	18 May 1994	H α	1950	4a
WR75	19 May 1994	[OIII]	2100	4b
WR75	17 May 1994	H α	2700	1a
WR85	17 May 1994	[OIII]	2700	1b
WR85	16 May 1994	H α	900	5

* uses the nomenclature of van der Hucht et al. (1981).

ejection events. This uses a similar line of argument to that proposed by Balick *et al.* (1992) for using the extended halos of planetary nebulae to distinguish the characteristics of the red giant stellar winds that existed prior to their formation.

In this paper, we provide new, deep imaging of a number of multiple rings observed around WR stars in an optical narrow-band survey made of WR stars in the southern skies. We discuss their possible implications for WR evolution and postulate what further information they may provide about the evolution of massive stars with closer investigation.

2. OBSERVATIONS

Narrow-band imaging, using H α ($\lambda=6563 \text{ \AA}$, $\Delta\lambda=12 \text{ \AA}$) and [O III] ($\lambda=5006 \text{ \AA}$, $\Delta\lambda=44 \text{ \AA}$) filters was performed using a Thomson 1024 \times 1024 CCD chip at the $f/3$ focus of the 0.6 m Curtis Schmidt at Cerro Tololo Interamerican Observatory (CTIO) during the nights of 15–19 May 1994. The sample objects were taken from the lists of Marston *et al.* (1994) and Marston & Yocom (in preparation). It was intended that all possible shells associated with the WR stars would be identified as well as information on relative sizes and morphologies. A full listing of observations used in this paper are supplied in Table 1.

3. RESULTS ON MULTIPLE RINGS

Images of the multiple ring systems of our sample are shown in Figs 1(a) and 1(b). These images allow us to study the bipolar shapes of the nebulae and apparent sizes of the multiple shells.

Fig Caption

Fig 1. (a) H α image of the filamentary, bipolar nebula RCW104 surrounding the WR star WR75. (b) Deep [O III] image of the wind-blown bubble at the center of RCW104.

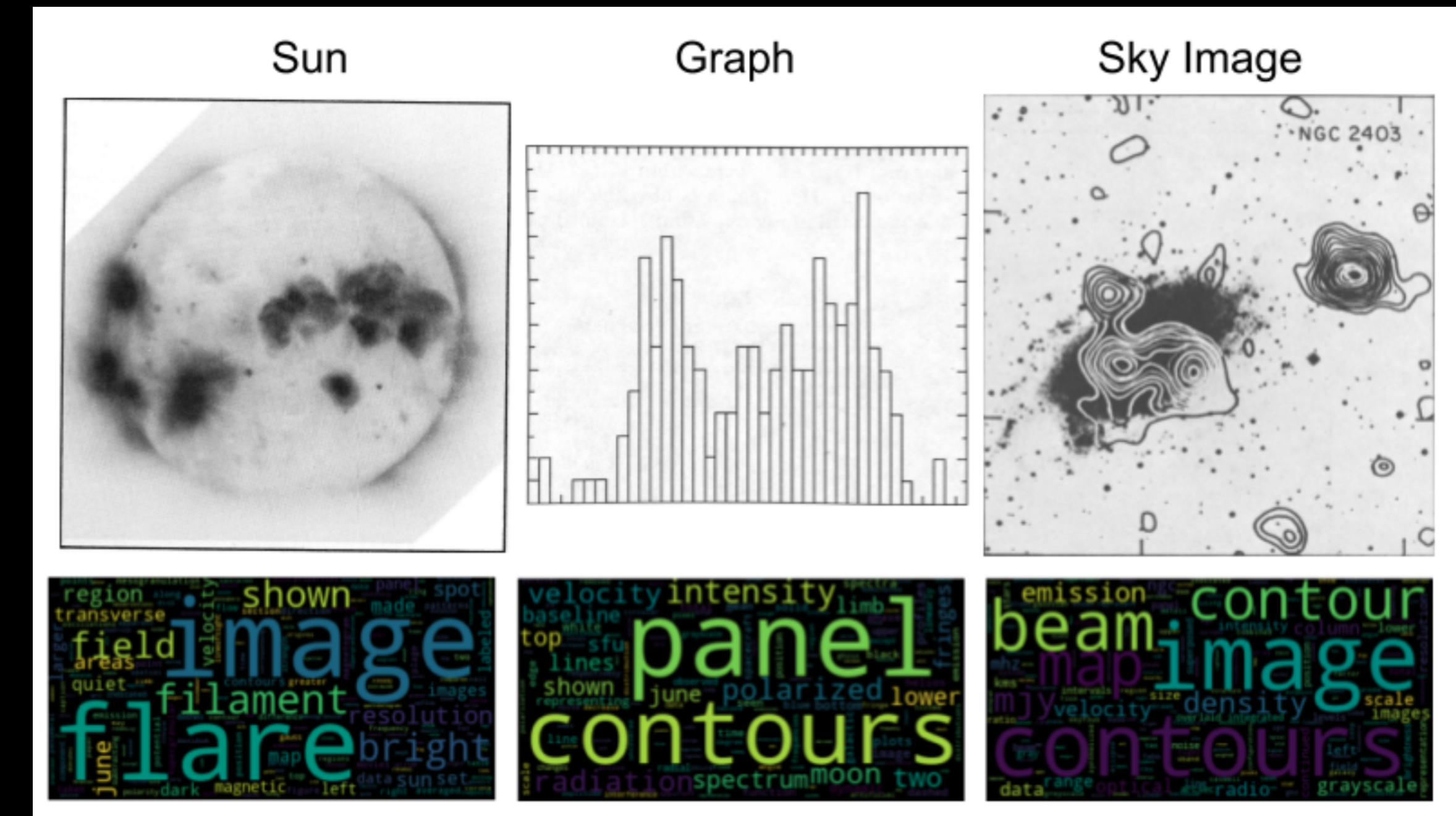
3.1 Bipolar Shells

Figures 1(a) and 1(b) show new, deep images of the nebula RCW 104 in both H α and [O III] which surrounds the WR star WR75. This is the only object in our sample to show a bipolar morphology in H α . However, close inspection of Fig. 1 of Marston *et al.* (1994) shows that the nebula NGC 2359 around the star WR6 has a diffuse outer, bipolar shell, which extends to approximately $20'$ from the central star. The bright shell in the center is only $5'$ across. NGC 2359 has been shown to have multiple velocity components which may be associated with multiple ejections (Goudis *et al.* 1994). Ejected material appears to be interacting with the diffuse bipolar materials as well as a nearby molecular cloud (Marston 1991; Schneps *et al.* 1981). The shell around

WR75 shows similar multiple components. An outer bipolar flow is outlined by strong H α filaments in the central regions while fainter lobes are observed to the north and south, extending to around $15'$ from the central WN6 star. An inner ring of [O III] emitting material is observed entirely within the bipolar outflow and is only $10'$ in diameter. The outer filaments of RCW 104 have been spectroscopically observed by Esteban *et al.* (1990), who suggest their abundances are similar to that expected from the enhanced abundances in a RSG wind. We might interpret our observation of these two bipolar nebulae as being the RSG ejecta outer filaments and relatively young WR winds interacting with the ejecta to form central cavities. The expansion of the cavities has not yet reached the edge of the RSG ejecta.

In both cases of bipolar morphology, a wind-blown (W)

© American Astronomical Society • Provided by the NASA Astrophysics Data System



Jill P. Naiman

+ Peter Williams & Alyssa Goodman (Harvard, Seamless Astronomy)

+ Ishita Ghosh, Toby Tao, Shantanu Pagare, Ayesha Baweja, Linh Pham (iSchool)

TABLE 1. Multiple ring nebulae observed.					
WR star*	ID Number	Date observed	Filter	Exposure (secs)	Figure
WR16	HD86161	16 May 1994	H α	1800	2
WR30	HD94005	15 May 1994	H α	900	3a
WR40	HD96548	18 May 1994	H α	1950	3b
WR40		19 May 1994	[OIII]	2100	4b
WR75	HD14749	17 May 1994	H α	1700	1a
WR75	HD14749	17 May 1994	[OIII]	2700	1b
WR88	HR6392B	16 May 1994	H α	900	5

* uses the nomenclature of van der Hucht et al. (1988).

ejection events. This uses a similar line of argument to that proposed by Balick *et al.* (1992) for using the extended halos of planetary nebulae to distinguish the characteristics of the red giant stellar winds that existed prior to their formation.

In this paper, we provide new, deep imaging of a number of multiple rings observed around WR stars in an optical narrow-band survey made of WR stars in the southern skies. We discuss their possible implications for WR evolution and postulate what further information they may provide about the evolution of massive stars with closer investigation.

2. OBSERVATIONS

Narrow-band imaging, using H α ($\lambda=6563\text{ \AA}$, $\Delta\lambda=12\text{ \AA}$) and [O III] ($\lambda=5007\text{ \AA}$, $\Delta\lambda=44\text{ \AA}$) was performed using a Thermo 1024x1024 CCD chip at the $f/3$ focus of the 1.5 m Curtis Schmidt at Cerro Tololo Inter-American Observatory (CTIO) during the nights of 15–19 May 1994. The sample objects were taken from the lists of Marston *et al.* (1994) and Marston & Yocom (in preparation). It was intended that all possible shells associated with the WR stars would be identified as well as information on relative sizes and morphologies. A full listing of observations used in this paper are supplied in Table 1.

3. RESULTS ON MULTIPLE RINGS

Images of the multiple ring systems of our sample are shown in Figs. 1–5. These reveal nebulae whose morphologies allow a classification into two distinct types. Those with bipolar shapes in an outer ejecta shell, and those with more spherical outer shells. Table 2 lists the ring type (after Chu 1991) and apparent sizes of the multiple shells.

3.1 Bipolar Shells

WR75 shows similar multiple components. An outer bipolar flow is outlined by strong H α filaments in the central regions while fainter lobes are observed to the north and south, extending to around $15'$ from the central WN9 star. An inner ring of [O III] emitting material is observed entirely within the bipolar outflow and is only $10'$ in diameter. The outer filaments of RCW104 have been spectroscopically observed by Esteban *et al.* (1990), who suggest their abundances are similar to those expected from the enhanced abundances in a RSG wind. We might interpret our observations of these two bipolar nebulae as being RSG ejected outer filaments and relatively young WR winds interacting with the ejecta to form central cavities. The expansion of the cavities has not yet reached the edge of the RSG ejecta.

In both cases of bipolar morphology, a wind-blown (W)

© American Astronomical Society • Provided by the NASA Astrophysics Data System

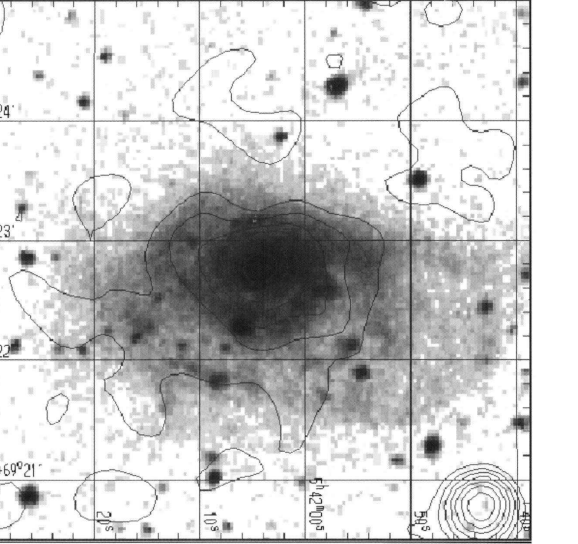


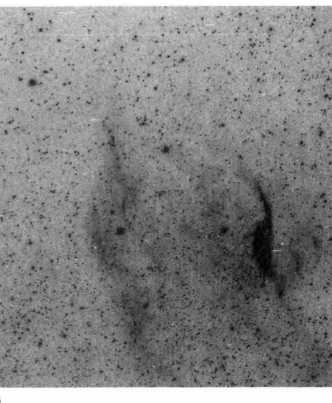
FIG. 1. The HRI data (contours) are overlaying the optical image of NGC 1961 from the digitized sky survey. The X-ray data have been smoothed with a Gaussian with $\sigma=10''$ and the contour levels are $(6.66, 7.77, 8.88, 9.98, 11.09, 12.20, 13.31, 14.42, 15.53, 16.64) \times 10^{-2} \text{ counts s}^{-1} \text{ arcmin}^{-2}$.

$37''$ centered on the peak of the emission from the northwest quadrant of the galaxy, we determine the count rate is $5.58 \times 10^{-3} \pm 0.73 \times 10^{-3} \text{ counts s}^{-1}$, which corresponds to an X-ray luminosity of $7.26 \times 10^{41} \text{ erg s}^{-1}$. The count rate from the nuclear region is $2.58 \times 10^{-3} \pm 0.32 \times 10^{-3} \text{ counts s}^{-1}$ which corresponds to an X-ray luminosity of $3.2 \times 10^{41} \text{ erg s}^{-1}$ in a $22''$ circular aperture. This implies that the X-ray luminosity from the disk of this galaxy is at least $7.9 \times 10^{41} \text{ erg s}^{-1}$.

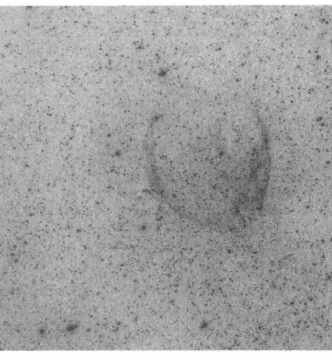
3. OPTICAL DATA

Images in a variety of passbands and spectral data were acquired for both galaxies to trace both young and old stellar components. Narrow-band images, with filters (of typical bandwidth 60 \AA) isolating H β , [O III] $\lambda 5007$, H α +[N II] $\lambda 6583$, and [S II] $\lambda\lambda 6717$ – 6731 at each galaxy's redshift, along with adjacent continuum bands at 5125 and 6694 \AA for continuum subtraction, were obtained at the KPNO 2.1 m telescope with the video-camera system in 1984 October. The field of view was 140 arcsec, well matched to the size of NGC 2276 and requiring two pointings for NGC 1961 (so that only the central part was observed in the H β , [O III], and [S II] passbands). Additional broad-band images were obtained with CCDs for NGC 2276 (in B at the KPNO 2.1 m and $BVRI$ at the Lowell 1.1 m) and NGC 1961 ($BVRI$ and narrow band for H α). The Video Camera data used a combination of internal quartz and night-sky flat fields, with geometric distortions produced by the image-tube chain corrected after flat-field division. Since it corrects to constant

© American Astronomical Society • Provided by the NASA Astrophysics Data System



(a)



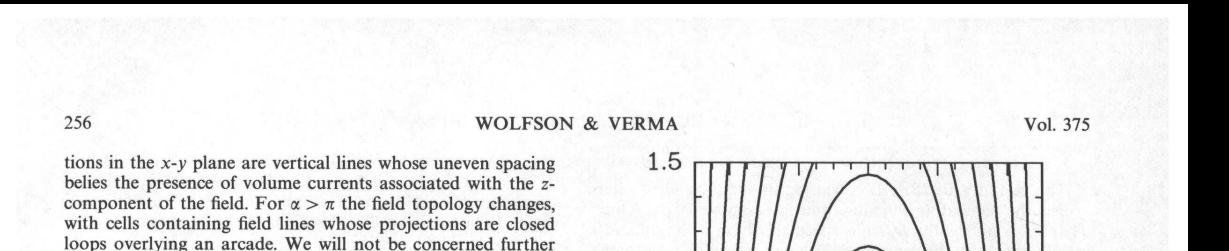
(b)

Fig. 1. (a) H α image of the filamentary, bipolar nebula RCW104 surrounding the WR star WR75. (b) Deep [O III] image of the wind-blown bubble at the center of RCW104.

WR75 shows similar multiple components. An outer bipolar flow is outlined by strong H α filaments in the central regions while fainter lobes are observed to the north and south, extending to around $15'$ from the central WN9 star. An inner ring of [O III] emitting material is observed entirely within the bipolar outflow and is only $10'$ in diameter. The outer filaments of RCW104 have been spectroscopically observed by Esteban *et al.* (1990), who suggest their abundances are similar to those expected from the enhanced abundances in a RSG wind. We might interpret our observations of these two bipolar nebulae as being RSG ejected outer filaments and relatively young WR winds interacting with the ejecta to form central cavities. The expansion of the cavities has not yet reached the edge of the RSG ejecta.

In both cases of bipolar morphology, a wind-blown (W)

© American Astronomical Society • Provided by the NASA Astrophysics Data System



256

WOLFSON & VERMA

Vol. 375

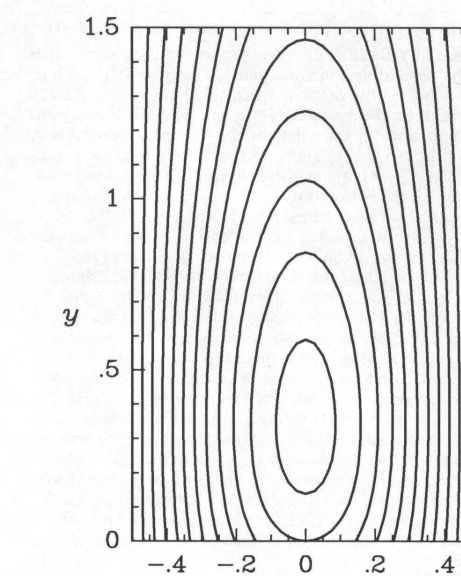


Fig. 3.—Field lines projected into the x - y plane for the nonlinear solution $A = A_0 + eA_1$, with $e = 0.2$ and $x = 3.02$. In this case the current enhancement is greater than to leave the x - y plane, a situation which would be impossible in the temporal evolution of an ideal MHD system. Although this figure illustrates qualitatively what a closed-loop solution looks like, the assumptions leading to the perturbation expansion $A = A_0 + eA_1$ are violated before closed loops appear (see Fig. 4).

$$\Delta z(x_f) = \frac{2x}{\sqrt{x^2 - x^2}} x_f = \lambda x_f, \quad (9)$$

where we have defined λ by

$$\lambda \equiv \frac{2x}{\sqrt{x^2 - x^2}}. \quad (10)$$

Thus the shear is a simple linear function of footpoint location, a fact shown graphically in Priest (1982, Fig. 3.8) and again in our Figure 5.

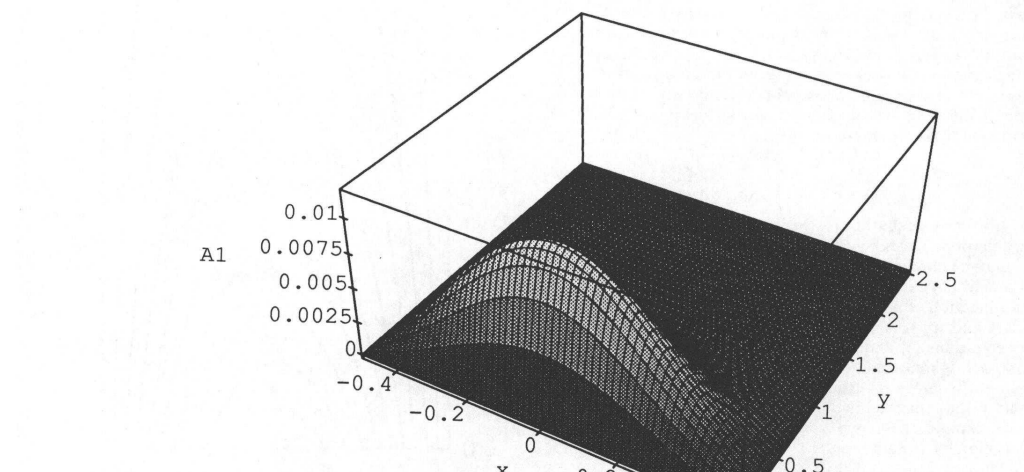


Fig. 2.—Plot of the perturbation solution $A_1(x, y)$, for $x = 0.5$. The single maximum corresponds to a region where current density is enhanced over the constant- x solution.

© American Astronomical Society • Provided by the NASA Astrophysics Data System

The Dataset

to which it is subject in consequence of the attraction of the sun and moon and as modified by the resulting distortion of the body of the earth. But this may be furnished with any desired degree of accuracy by the changes in the position of the level of a liquid surface which is necessarily normal to the resultant of all the forces acting. If from these we can eliminate all but the gravitational forces the problem is solved.

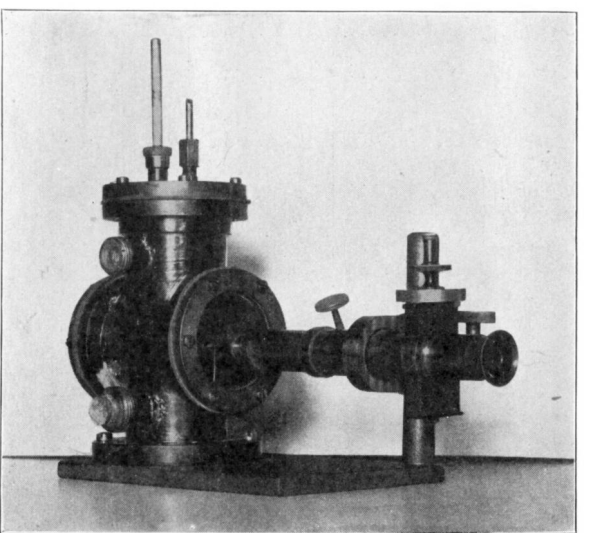


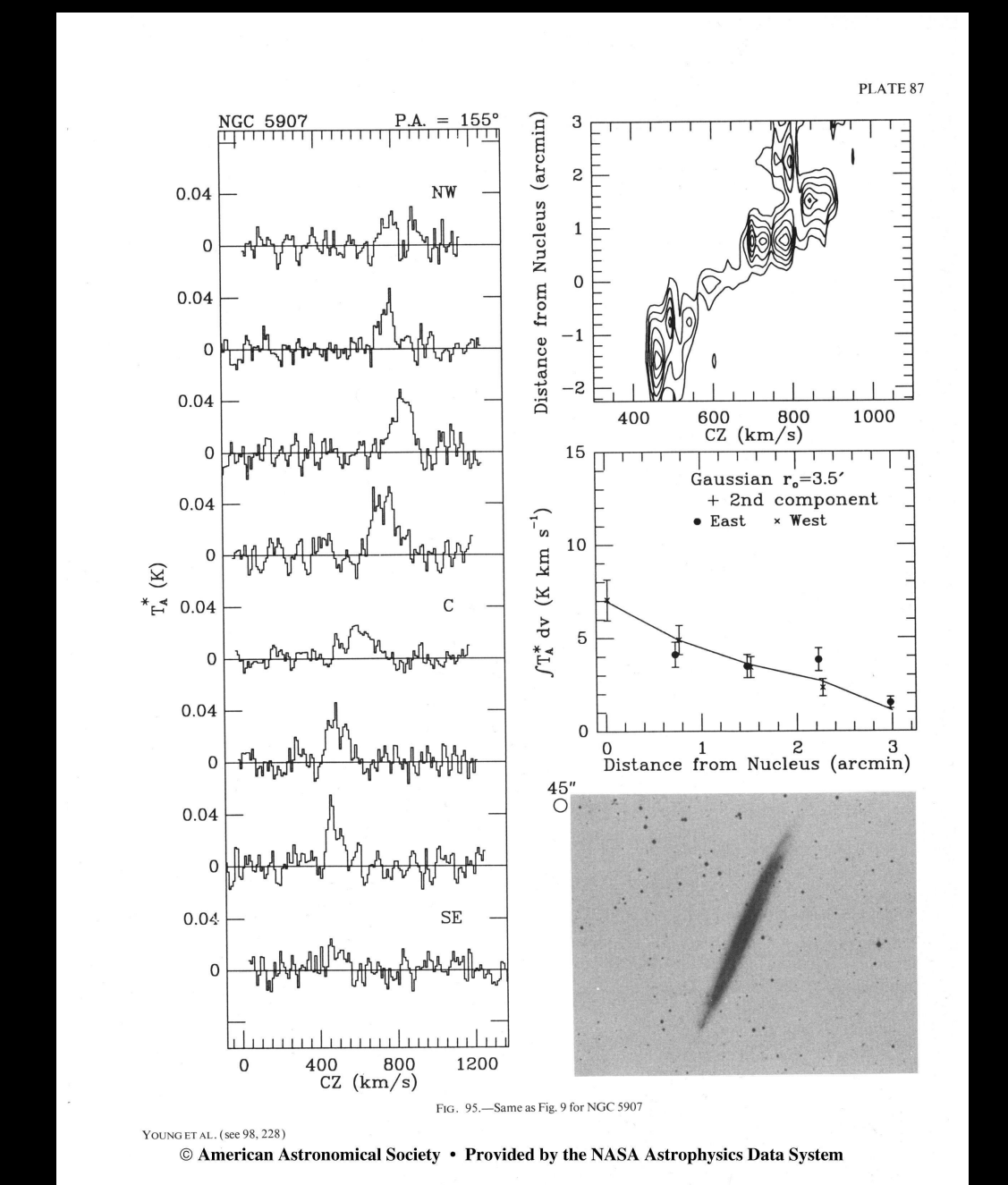
FIG. 1.—Microscope and gauge

A very sensitive method of measuring the changes in level is furnished by the interferometer; and a method of carrying this into practice was devised and the apparatus constructed¹ in 1910.

But before attempting to utilize so delicate an appliance it was deemed advisable to make these preliminary experiments with the microscope. Accordingly a 6-inch pipe, 500 feet long, was half filled with water,² the level of which could be read off through the glass sides of the end vessels, as shown in Fig. 1.

¹ An interference apparatus for this purpose was independently devised by Professor A. G. Webster.

² The vessels at the ends were at first connected by a pipe filled with water, but with this arrangement temperature changes produced enormous disturbances in the level.



YOUNG ET AL. (see 98, 228)
© American Astronomical Society • Provided by the NASA Astrophysics Data System

FIG. 95.—Same as Fig. 9 for NGC 5907

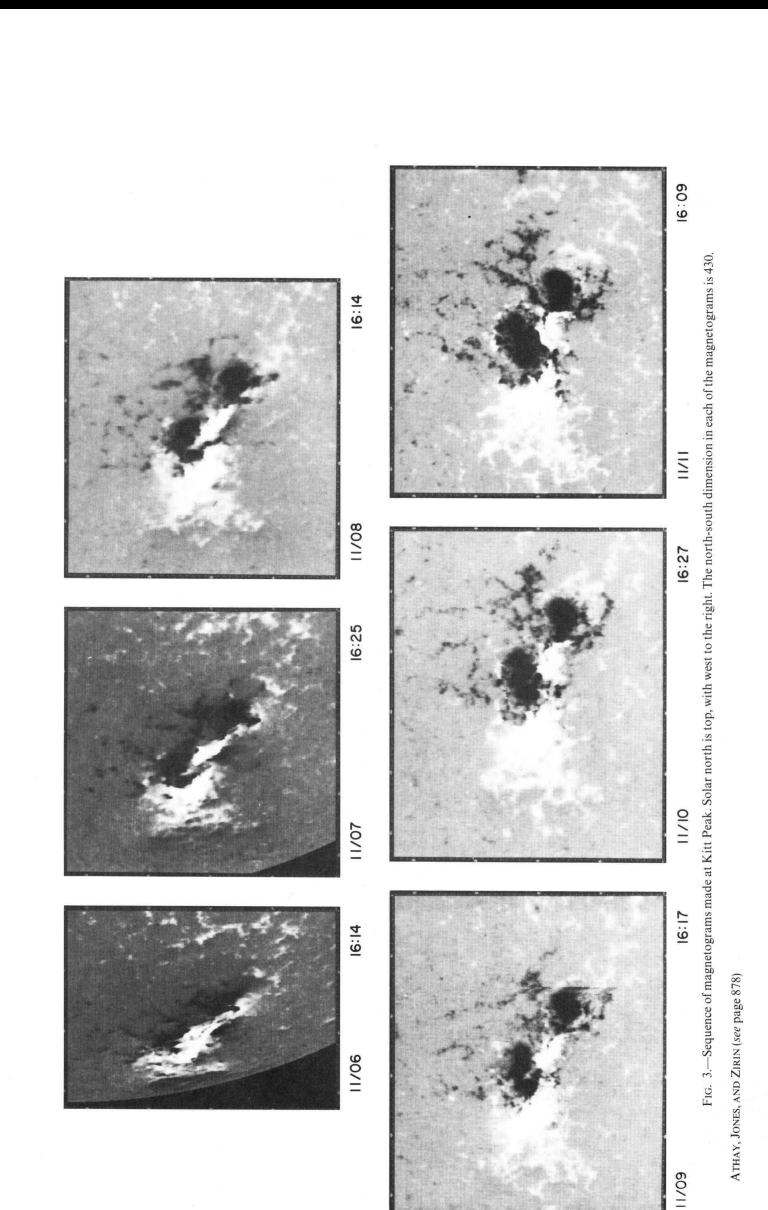


FIG. 3.—Sequence of magnetograms made at Kitt Peak. Solar north is top; west to the right. The north-south dimension in each of the magnetograms is $\pm 30^\circ$.
ATHANASIOS AND ZAHLER (see page 878)

The Dataset

The Astrophysics Data System (ADS): <https://ui.adsabs.harvard.edu/>

The screenshot shows the ADS search interface with the query 'naiman' entered. The search returned 42 results.

Left Sidebar:

- AUTHORS:**
 - > Naiman, J 42
 - > Hernquist, L 16
 - > Springel, V 16
 - > Vogelsberger, M 16
 - > Marinacci, F 15
- COLLECTIONS:**
 - astronomy 41
 - physics 3
 - general 2
- REFEREED:**
 - refereed 31
 - non-refereed 11
- INSTITUTIONS**
- KEYWORDS**
- PUBLICATIONS**
- BIB GROUPS**

Search Bar: QUICK FIELD: Author First Author Abstract Year Fulltext All Search Terms

Search Results:

- 1 2020arXiv201011227B 2020/10 cited: 1 [The Catalogue for Astrophysical Turbulence Simulations \(CATS\)](#) Burkhardt, B.; Appel, S.; Bialy, S. *and 18 more*
- 2 2020A&C....3300424A 2020/10 [Clustering-informed cinematic astrophysical data visualization with application to the Moon-forming terrestrial synestia](#) Aleo, P. D.; Lock, S. J.; Cox, D. J. *and 5 more*
- 3 2020ApJ...899L..30G 2020/08 cited: 2 [Winds in Star Clusters Drive Kolmogorov Turbulence](#) Gallegos-Garcia, Monica; Burkhardt, Blakesley; Rosen, Anna L. *and 2 more*
- 4 2020ApJ...896...66K 2020/06 cited: 1 [The Effects of Metallicity and Abundance Pattern of the ISM on Supernova Feedback](#) Karpov, Platon I.; Martizzi, Davide; Macias, Phillip *and 3 more*
- 5 2020MNRAS.492.5930L 2020/03 cited: 4 [Redshift evolution of the Fundamental Plane relation in the IllustrisTNG simulation](#) Lu, Shengdong; Xu, Dandan; Wang, Yunchong *and 7 more*

Right Sidebar:

- Add papers to library**
- Create email notification**
- Years** **Citations** **Reads**
- refereed** **non refereed**

The Idea

TABLE 1. Multiple ring nebulae observed.

WR star ^a	HD Number	Date observed	Filter	Exposure (secs)	Figure
WR16	HD86161	16 May 1994	H α	1800	2
WR30	HD94305	15 May 1994	H α	900	3a
WR30	-	19 May 1994	[OIII]	2100	3b
WR40	HD96548	18 May 1994	H α	1950	4a
WR40	-	19 May 1994	[OIII]	2100	4b
WR75	HD14749	17 May 1994	H α	2700	1a
WR75	-	17 May 1994	[OIII]	2700	1b
WR85	HR6392B	16 May 1994	H α	900	5

^a uses the nomenclature of van der Hucht *et al.* (1981).

ejection events. This uses a similar line of argument to that proposed by Balick *et al.* (1992) for using the extended halos of planetary nebulae to distinguish the characteristics of the red giant stellar winds that existed prior to their formation.

In this paper, we provide new, deep imaging of a number of multiple rings observed around WR stars in an optical narrow-band survey made of WR stars in the southern skies. We discuss their possible implications for WR evolution and postulate what further information they may provide about the evolution of massive stars with closer investigation.

2. OBSERVATIONS

Narrow-band imaging, using H α ($\lambda=6563\text{ \AA}$, $\Delta\lambda=12\text{ \AA}$) and [O III] ($\lambda=5006\text{ \AA}$, $\Delta\lambda=44\text{ \AA}$) filters was performed using a Thomson 1024×1024 CCD chip at the f/3 focus of the 0.6 m Curtis Schmidt at Cerro Tololo Interamerican Observatory (CTIO) during the nights of 15–19 May 1994. The sample objects were taken from the lists of Marston *et al.* (1994) and Marston & Yocum (in preparation). It was intended that all possible shells associated with the WR stars would be identified as well as information on relative sizes and morphologies. A full listing of observations used in this paper are supplied in Table 1.

3. RESULTS ON MULTIPLE RINGS

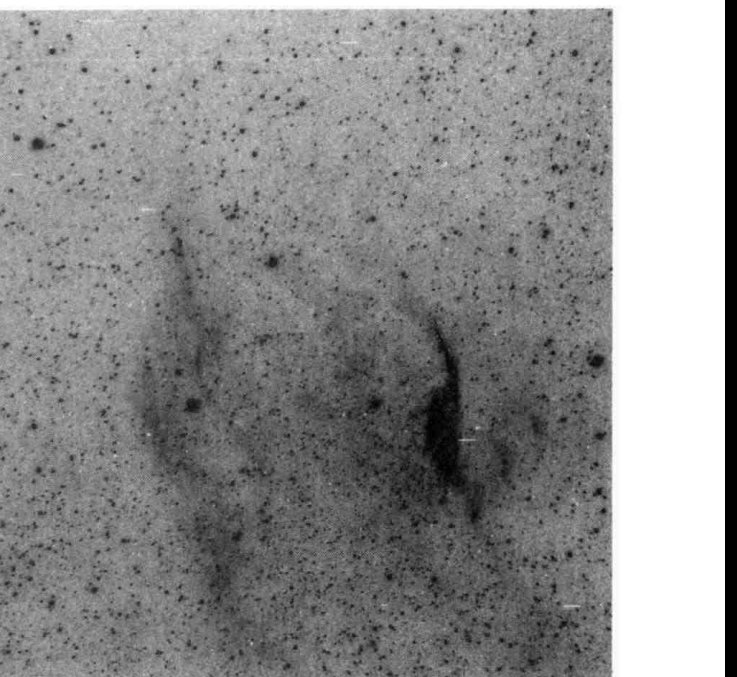
Images of the multiple ring systems of our sample are shown in Figs. 1–5. These reveal nebulae whose morphologies allow a classification into two distinct types. Those with bipolar shapes in an outer ejecta shell, and those with more spherical outer shells. Table 2 lists the ring type (after Chu 1991) and apparent sizes of the multiple shells.

3.1 Bipolar Shells

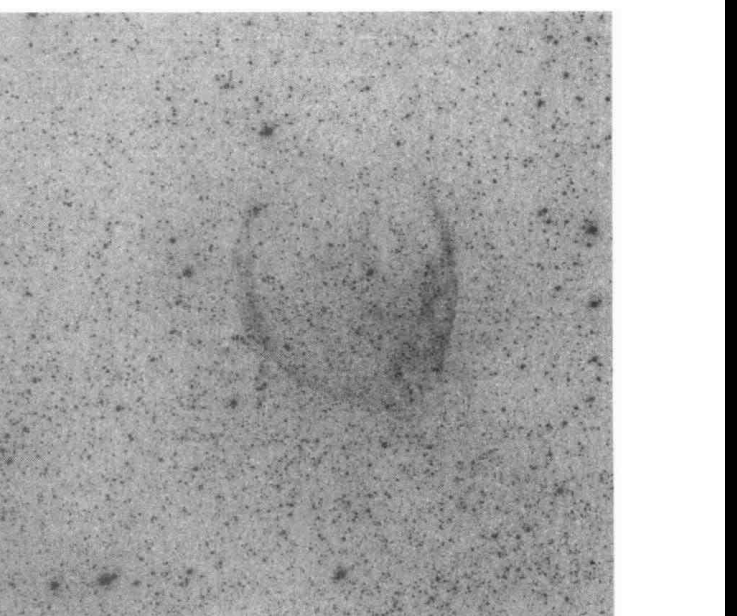
Figures 1(a) and 1(b) show new, deep images of the nebula RCW 104 in both H α and [O III] which surrounds the WR star WR75. This is the only object in our sample to show a bipolar morphology in H α . However, close inspection of Fig. 1 of Marston *et al.* (1994) shows that the nebula NGC 2359 around the star WR6 has a diffuse outer, bipolar shell, which extends to approximately 20' from the central star. The bright shell in the center is only 5' across. NGC 2359 has been shown to have multiple velocity components which may be associated with multiple ejections (Goudis *et al.* 1994). Ejected material appears to be interacting with the diffuse bipolar materials as well as a nearby molecular cloud (Marston 1991; Schneps *et al.* 1981). The shell around

WR75 shows similar multiple components. An outer bipolar flow is outlined by strong H α filaments in the central regions while fainter lobes are observed to the north and south, extending to around 15' from the central WN6 star. An inner ring of [O III] emitting material is observed entirely within the bipolar outflow and is only 10' in diameter. The outer filaments of RCW 104 have been spectroscopically observed by Esteban *et al.* (1990), who suggest their abundances are similar to that expected from the enhanced abundances in a RSG wind. We might interpret our observations of these two bipolar nebulae as being the RSG ejecta outer filaments and relatively young WR winds interacting with the ejecta to form central cavities. The expansion of the cavities has not yet reached the edge of the RSG ejecta.

In both cases of bipolar morphology, a wind-blown (W)



(a)



(b)

FIG. 1. (a) H α image of the filamentary, bipolar nebula RCW104 surrounding the WR star WR75. (b) Deep [O III] image of the wind-blown bubble at the center of RCW104.

The Idea

1840 A. R. MARSTON: RINGS AROUND WR STARS

TABLE 1. Multiple ring nebulae observed.						
WR star ^a	HD Number	Date observed	Filter	Exposure (secs)	Figure	
WR16	HD86161	16 May 1994	H α	1800	2	
WR30	HD94305	15 May 1994	H α	900	3a	
WR30	-	19 May 1994	[OIII]	2100	3b	
WR40	HD96548	18 May 1994	H α	1950	4a	
WR40	-	19 May 1994	[OIII]	2100	4b	
WR75	HD14749	17 May 1994	H α	2700	1a	
WR75	-	17 May 1994	[OIII]	2700	1b	
WR85	HR6392B	16 May 1994	H α	900	5	

^a uses the nomenclature of van der Hucht *et al.* (1981).

ejection events. This uses a similar line of argument to that proposed by Balick *et al.* (1992) for using the extended halos of planetary nebulae to distinguish the characteristics of the red giant stellar winds that existed prior to their formation.

In this paper, we provide new, deep imaging of a number of multiple rings observed around WR stars in an optical narrow-band survey made of WR stars in the southern skies. We discuss their possible implications for WR evolution and postulate what further information they may provide about the evolution of massive stars with closer investigation.

2. OBSERVATIONS

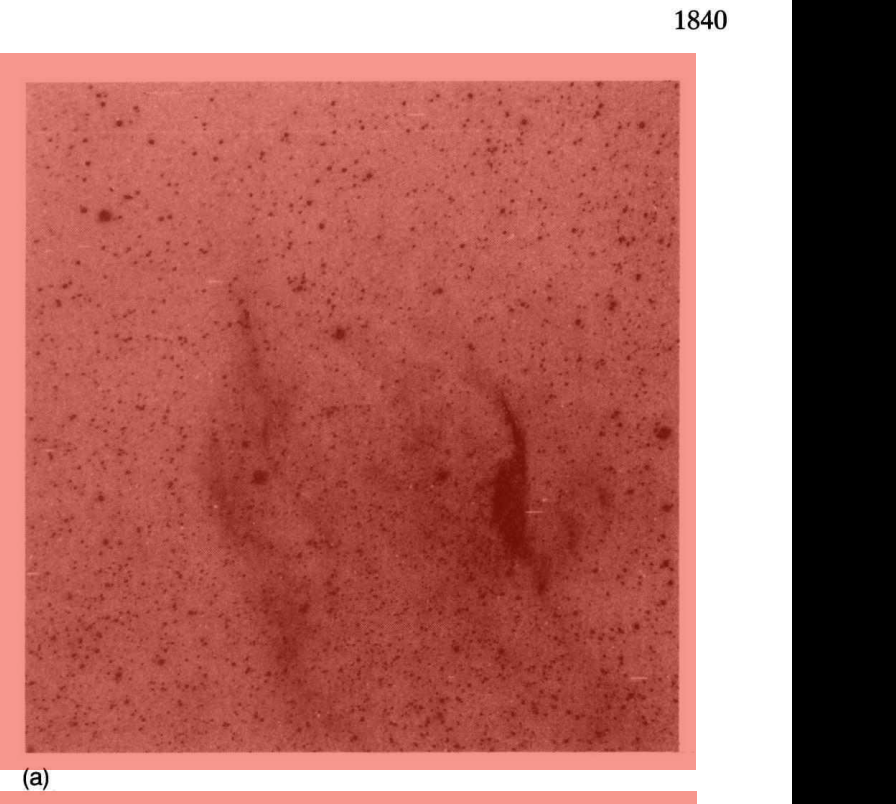
Narrow-band imaging, using H α ($\lambda=6563\text{ \AA}$, $\Delta\lambda=12\text{ \AA}$) and [O III] ($\lambda=5006\text{ \AA}$, $\Delta\lambda=44\text{ \AA}$) filters was performed using a Thomson 1024 \times 1024 CCD chip at the f/3 focus of the 0.6 m Curtis Schmidt at Cerro Tololo Interamerican Observatory (CTIO) during the nights of 15–19 May 1994. The sample objects were taken from the lists of Marston *et al.* (1994) and Marston & Yocum (in preparation). It was intended that all possible shells associated with the WR stars would be identified as well as information on relative sizes and morphologies. A full listing of observations used in this paper are supplied in Table 1.

3. RESULTS ON MULTIPLE RINGS

Images of the multiple ring systems of our sample are shown in Figs. 1–5. These reveal nebulae whose morphologies allow a classification into two distinct types. Those with bipolar shapes in an outer ejecta shell, and those with more spherical outer shells. Table 2 lists the ring type (after Chu 1991) and apparent sizes of the multiple shells.

3.1 Bipolar Shells

Figures 1(a) and 1(b) show new, deep images of the nebula RCW 104 in both H α and [O III] which surrounds the WR star WR75. This is the only object in our sample to show a bipolar morphology in H α . However, close inspection of Fig. 1 of Marston *et al.* (1994) shows that the nebula NGC 2359 around the star WR6 has a diffuse outer, bipolar shell, which extends to approximately 20' from the central star. The bright shell in the center is only 5' across. NGC 2359 has been shown to have multiple velocity components which may be associated with multiple ejections (Goudis *et al.* 1994). Ejected material appears to be interacting with the diffuse bipolar materials as well as a nearby molecular cloud (Marston 1991; Schneps *et al.* 1981). The shell around



1840

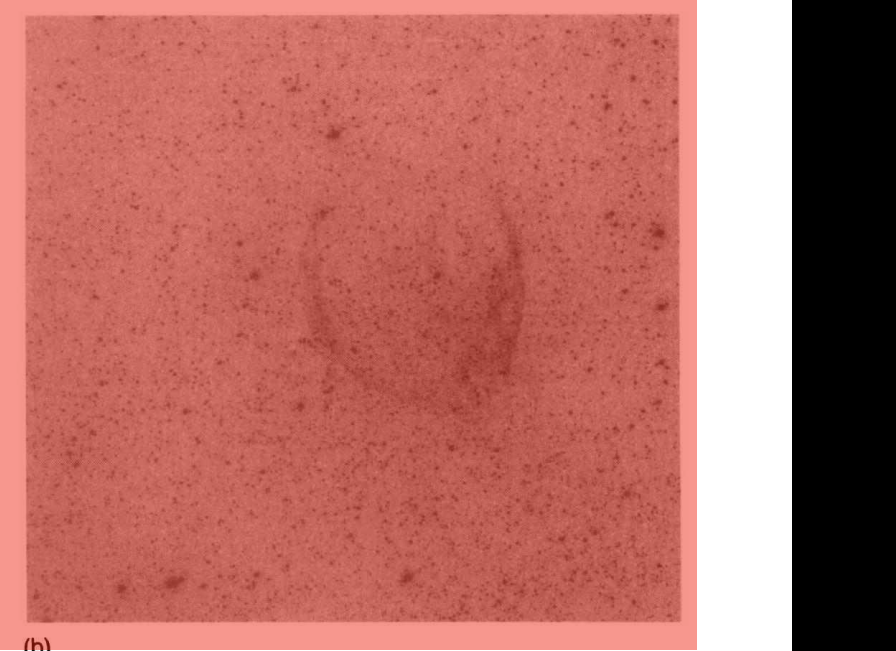


FIG. 1. (a) H α image of the filamentary, bipolar nebula RCW104 surrounding the WR star WR75. (b) Deep [O III] image of the wind-blown bubble at the center of RCW104.

WR75 shows similar multiple components. An outer bipolar flow is outlined by strong H α filaments in the central regions while fainter lobes are observed to the north and south, extending to around 15' from the central WN6 star. An inner ring of [O III] emitting material is observed entirely within the bipolar outflow and is only 10' in diameter. The outer filaments of RCW 104 have been spectroscopically observed by Esteban *et al.* (1990), who suggest their abundances are similar to that expected from the enhanced abundances in a RSG wind. We might interpret our observations of these two bipolar nebulae as being the RSG ejecta outer filaments and relatively young WR winds interacting with the ejecta to form central cavities. The expansion of the cavities has not yet reached the edge of the RSG ejecta.

In both cases of bipolar morphology, a wind-blown (W)

The Idea

1840 A. R. MARSTON: RINGS AROUND WR STARS

Table 1. Multiple ring nebulae observed.					
	Number	Date observed	Filter	Exposure (secs)	Figure
WR30	HD94305	16 May 1994	H α	1800	2
WR30	-	15 May 1994	H α	900	3a
WR40	HD96548	19 May 1994	[OIII]	2100	3b
WR40	-	18 May 1994	H α	1950	4a
WR75	-	19 May 1994	[OIII]	2100	4b
WR75	HD14749	17 May 1994	H α	2700	1a
WR75	-	17 May 1994	[OIII]	2700	1b
WR85	HR6392B	16 May 1994	H α	900	5

^a uses the nomenclature of van der Hucht *et al.* (1981).

ejection events. This uses a similar line of argument to that proposed by Balick *et al.* (1992) for using the extended halos of planetary nebulae to distinguish the characteristics of the red giant stellar winds that existed prior to their formation.

In this paper, we provide new, deep imaging of a number of multiple rings observed around WR stars in an optical narrow-band survey made of WR stars in the southern skies. We discuss their possible implications for WR evolution and postulate what further information they may provide about the evolution of massive stars with closer investigation.

2. OBSERVATIONS

Narrow-band imaging, using H α ($\lambda=6563\text{ \AA}$, $\Delta\lambda=12\text{ \AA}$) and [O III] ($\lambda=5006\text{ \AA}$, $\Delta\lambda=44\text{ \AA}$) filters was performed using a Thomson 1024 \times 1024 CCD chip at the f/3 focus of the 0.6 m Curtis Schmidt at Cerro Tololo Interamerican Observatory (CTIO) during the nights of 15–19 May 1994. The sample objects were taken from the lists of Marston *et al.* (1994) and Marston & Yocum (in preparation). It was intended that all possible shells associated with the WR stars would be identified as well as information on relative sizes and morphologies. A full listing of observations used in this paper are supplied in Table 1.

3. RESULTS ON MULTIPLE RINGS

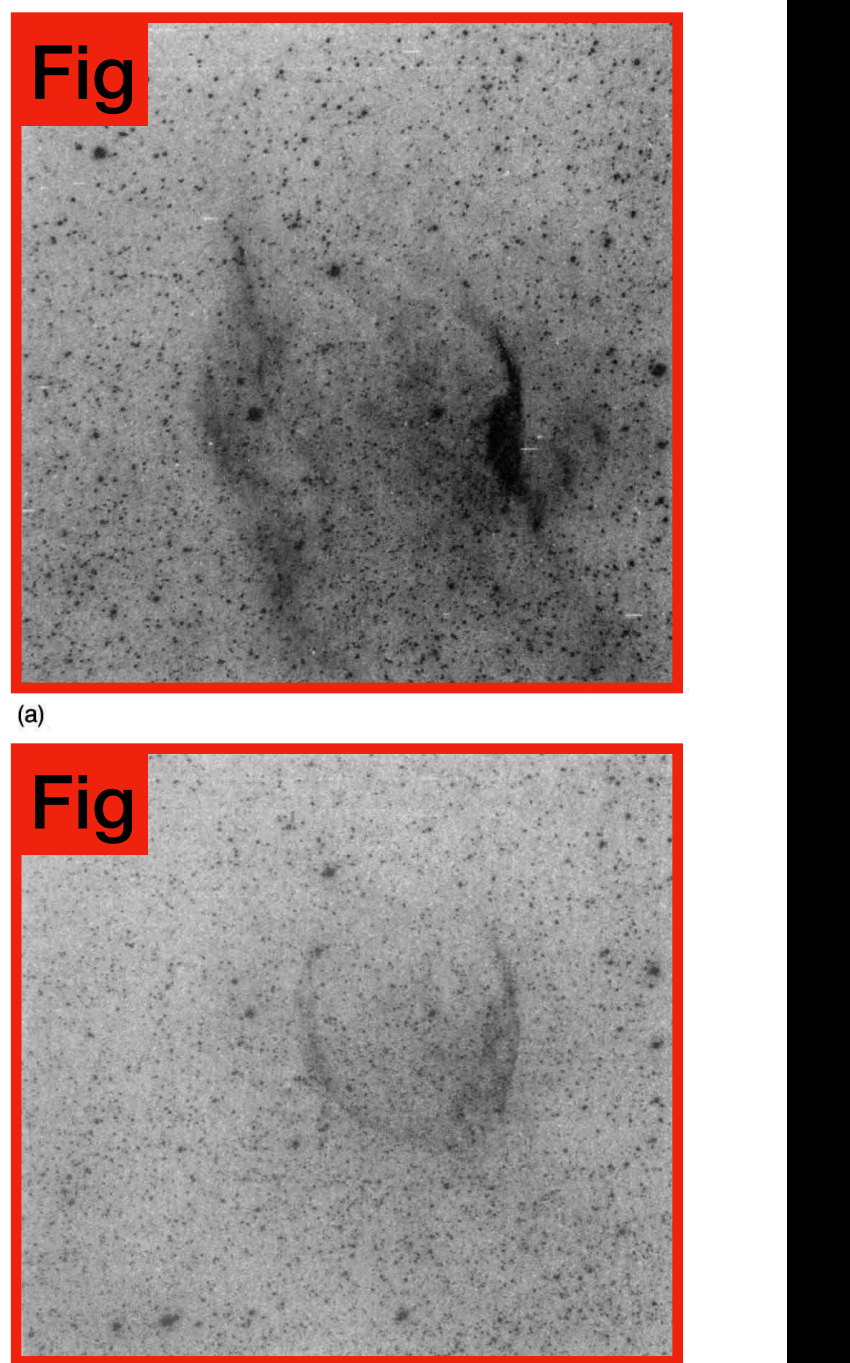
Images of the multiple ring systems of our sample are shown in Figs. 1–5. These figures allow a classification in Fig. 1. (a) H α image of the filamentary, bipolar nebula RCW104 surrounding the WR star WR75. (b) Deep [O III] image of the wind-blown bubble at the center of RCW104.

Fig Caption

spherical outer shells. Table 2 lists the ring type (after Chu 1991) and apparent sizes of the multiple shells.

3.1 Bipolar Shells

Figures 1(a) and 1(b) show new, deep images of the nebula RCW 104 in both H α and [O III] which surrounds the WR star WR75. This is the only object in our sample to show a bipolar morphology in H α . However, close inspection of Fig. 1 of Marston *et al.* (1994) shows that the nebula NGC 2359 around the star WR6 has a diffuse outer, bipolar shell, which extends to approximately 20' from the central star. The bright shell in the center is only 5' across. NGC 2359 has been shown to have multiple velocity components which may be associated with multiple ejections (Goudis *et al.* 1994). Ejected material appears to be interacting with the diffuse bipolar materials as well as a nearby molecular cloud (Marston 1991; Schneps *et al.* 1981). The shell around



1840

FIG. 1. (a) H α image of the filamentary, bipolar nebula RCW104 surrounding the WR star WR75. (b) Deep [O III] image of the wind-blown bubble at the center of RCW104.

WR75 shows similar multiple components. An outer bipolar flow is outlined by strong H α filaments in the central regions while fainter lobes are observed to the north and south, extending to around 15' from the central WN6 star. An inner ring of [O III] emitting material is observed entirely within the bipolar outflow and is only 10' in diameter. The outer filaments of RCW 104 have been spectroscopically observed by Esteban *et al.* (1990), who suggest their abundances are similar to that expected from the enhanced abundances in a RSG wind. We might interpret our observations of these two bipolar nebulae as being the RSG ejecta outer filaments and relatively young WR winds interacting with the ejecta to form central cavities. The expansion of the cavities has not yet reached the edge of the RSG ejecta.

In both cases of bipolar morphology, a wind-blown (W)

The Idea

1840 A. R. MARSTON: RINGS AROUND WR STARS

Table

Fig 1. Multiple ring nebulae observed.

Number	Date observed	Filter	Exposure (secs)	Figure	
61	16 May 1994	H α	1800	2	
WR30	HD94305	15 May 1994	H α	900	3a
WR30	-	19 May 1994	[OIII]	2100	3b
WR40	HD96548	18 May 1994	H α	1950	4a
WR40	-	19 May 1994	[OIII]	2100	4b
WR75	HD14749	17 May 1994	H α	2700	1a
WR75	-	17 May 1994	[OIII]	2700	1b
WR85	HR6392B	16 May 1994	H α	900	5

^a uses the nomenclature of van der Hucht et al. (1981).

ejection events. This uses a similar line of argument to that proposed by Balick *et al.* (1992) for using the extended halos of planetary nebulae to distinguish the characteristics of the red giant stellar winds that existed prior to their formation.

In this paper, we provide new, deep imaging of a number of multiple rings observed around WR stars in an optical narrow-band survey made of WR stars in the southern skies. We discuss their possible implications for WR evolution and postulate what further information they may provide about the evolution of massive stars with closer investigation.

2. OBSERVATIONS

Narrow-band imaging, using H α ($\lambda=6563 \text{ \AA}$, $\Delta\lambda=12 \text{ \AA}$) and [O III] ($\lambda=5006 \text{ \AA}$, $\Delta\lambda=44 \text{ \AA}$) filters was performed using a Thomson 1024×1024 CCD chip at the f/3 focus of the 0.6 m Curtis Schmidt at Cerro Tololo Interamerican Observatory (CTIO) during the nights of 15–19 May 1994. The sample objects were taken from the lists of Marston *et al.* (1994) and Marston & Yocum (in preparation). It was intended that all possible shells associated with the WR stars would be identified as well as information on relative sizes and morphologies. A full listing of observations used in this paper are supplied in Table 1.

3. RESULTS ON MULTIPLE RINGS

Images of the multiple ring systems of our sample are shown in Figs. 1–5. These figures allow a classification in Fig Caption bipolar shapes in an outer spherical outer shells. Table 2 lists the ring type (after Chu 1991) and apparent sizes of the multiple shells.

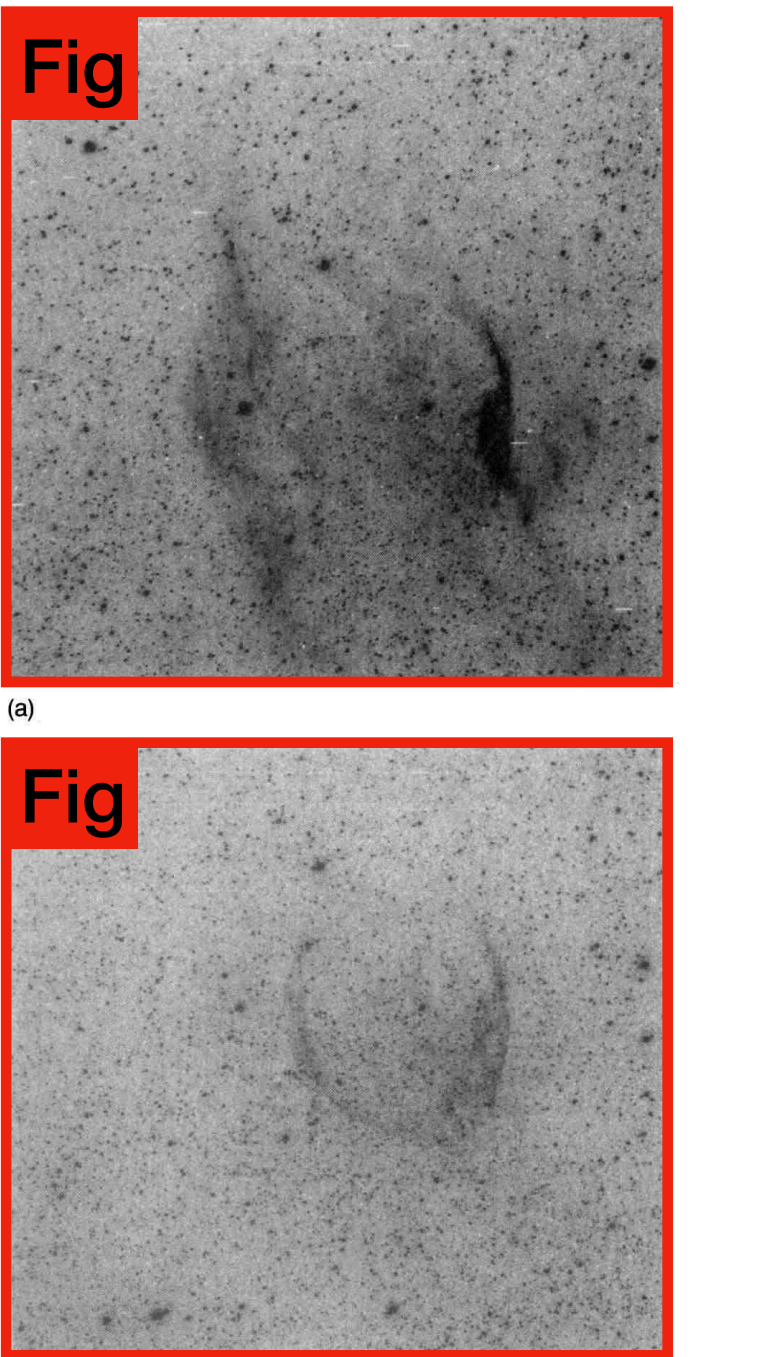
3.1 Bipolar Shells

Figures 1(a) and 1(b) show new, deep images of the nebula RCW 104 in both H α and [O III] which surrounds the WR star WR75. This is the only object in our sample to show a bipolar morphology in H α . However, close inspection of Fig. 1 of Marston *et al.* (1994) shows that the nebula NGC 2359 around the star WR6 has a diffuse outer, bipolar shell, which extends to approximately 20' from the central star. The bright shell in the center is only 5' across. NGC 2359 has been shown to have multiple velocity components which may be associated with multiple ejections (Goudis *et al.* 1994). Ejected material appears to be interacting with the diffuse bipolar materials as well as a nearby molecular cloud (Marston 1991; Schneps *et al.* 1981). The shell around

WR75 shows similar multiple components. An outer bipolar flow is outlined by strong H α filaments in the central regions while fainter lobes are observed to the north and south, extending to around 15' from the central WN6 star. An inner ring of [O III] emitting material is observed entirely within the bipolar outflow and is only 10' in diameter. The outer filaments of RCW 104 have been spectroscopically observed by Esteban *et al.* (1990), who suggest their abundances are similar to that expected from the enhanced abundances in a RSG wind. We might interpret our observations of these two bipolar nebulae as being the RSG ejecta outer filaments and relatively young WR winds interacting with the ejecta to form central cavities. The expansion of the cavities has not yet reached the edge of the RSG ejecta.

In both cases of bipolar morphology, a wind-blown (W)

FIG. 1. (a) H α image of the filamentary, bipolar nebula RCW104 surrounding the WR star WR75. (b) Deep [O III] image of the wind-blown bubble at the center of RCW104.



The Idea

1840 A. R. MARSTON: RINGS AROUND WR STARS

Table

Fig 1. Multiple ring nebulae observed.

Number	Date observed	Filter	Exposure (secs)	Figure	
61	16 May 1994	H α	1800	2	
WR30	HD94305	15 May 1994	H α	900	3a
WR30	-	19 May 1994	[OIII]	2100	3b
WR40	HD96548	18 May 1994	H α	1950	4a
WR40	-	19 May 1994	[OIII]	2100	4b
WR75	HD14749	17 May 1994	H α	2700	1a
WR75	-	17 May 1994	[OIII]	2700	1b
WR85	HR6392B	16 May 1994	H α	900	5

^a uses the nomenclature of van der Hucht et al. (1981).

ejection events. This uses a similar line of argument to that proposed by Balick *et al.* (1992) for using the extended halos of planetary nebulae to distinguish the characteristics of the red giant stellar winds that existed prior to their formation.

In this paper, we provide new, deep imaging of a number of multiple rings observed around WR stars in an optical narrow-band survey made of WR stars in the southern skies. We discuss their possible implications for WR evolution and postulate what further information they may provide about the evolution of massive stars with closer investigation.

2. OBSERVATIONS

Narrow-band imaging, using H α ($\lambda=6563 \text{ \AA}$, $\Delta\lambda=12 \text{ \AA}$) and [O III] ($\lambda=5006 \text{ \AA}$, $\Delta\lambda=44 \text{ \AA}$) filters was performed using a Thomson 1024 \times 1024 CCD chip at the f/3 focus of the 0.6 m Curtis Schmidt at Cerro Tololo Interamerican Observatory (CTIO) during the nights of 15–19 May 1994. The sample objects were taken from the lists of Marston *et al.* (1994) and Marston & Yocum (in preparation). It was intended that all possible shells associated with the WR stars would be identified as well as information on relative sizes and morphologies. A full listing of observations used in this paper are supplied in Table 1.

3. RESULTS ON MULTIPLE RINGS

Images of the multiple ring systems of our sample are shown in Figs. 1–5. These figures allow a classification in bipolar shapes in an outer spherical outer shells. Table 2 lists the ring type (after Chu 1991) and apparent sizes of the multiple shells.

3.1 Bipolar Shells

Figures 1(a) and 1(b) show new, deep images of the nebula RCW 104 in both H α and [O III] which surrounds the WR star WR75. This is the only object in our sample to show a bipolar morphology in H α . However, close inspection of Fig. 1 of Marston *et al.* (1994) shows that the nebula NGC 2359 around the star WR6 has a diffuse outer, bipolar shell, which extends to approximately 20' from the central star. The bright shell in the center is only 5' across. NGC 2359 has been shown to have multiple velocity components which may be associated with multiple ejections (Goudis *et al.* 1994). Ejected material appears to be interacting with the diffuse bipolar materials as well as a nearby molecular cloud (Marston 1991; Schneps *et al.* 1981). The shell around

Fig

(a)

Fig

(b)

Fig Caption

FIG. 1. (a) H α image of the filamentary, bipolar nebula RCW104 surrounding the WR star WR75. (b) Deep [O III] image of the wind-blown bubble at the center of RCW104.

WR75 shows similar multiple components. An outer bipolar flow is outlined by strong H α filaments in the central regions while fainter lobes are observed to the north and south, extending to around 15' from the central WN6 star. An inner ring of [O III] emitting material is observed entirely within the bipolar outflow and is only 10' in diameter. The outer filaments of RCW 104 have been spectroscopically observed by Esteban *et al.* (1990), who suggest their abundances are similar to that expected from the enhanced abundances in a RSG wind. We might interpret our observations of these two bipolar nebulae as being the RSG ejecta outer filaments and relatively young WR winds interacting with the ejecta to form central cavities. The expansion of the cavities has not yet reached the edge of the RSG ejecta.

In both cases of bipolar morphology, a wind-blown (W)

The Idea

1840 A. R. MARSTON: RINGS AROUND WR STARS

Table 1. Multiple ring nebulae observed.					
Number	Date observed	Filter	Exposure (secs)	Figure	
WR30	16 May 1994	H α	1800	2	
WR30	15 May 1994	H α	900	3a	
WR30	19 May 1994	[OIII]	2100	3b	
WR40	HD96548	H α	1950	4a	
WR40	-	[OIII]	2100	4b	
WR75	HD14749	H α	2700	1a	
WR75	-	[OIII]	2700	1b	
WR85	HR6392B	H α	900	5	

^a uses the nomenclature of van der Hucht *et al.* (1981).

ejection events. This uses a similar line of argument to that proposed by Balick *et al.* (1992) for using the extended halos of planetary nebulae to distinguish the characteristics of the red giant stellar winds that existed prior to their formation.

In this paper, we provide new, deep imaging of a number of multiple rings observed around WR stars in an optical narrow-band survey made of WR stars in the southern skies. We discuss their possible implications for WR evolution and postulate what further information they may provide about the evolution of massive stars with closer investigation.

2. OBSERVATIONS

Narrow-band imaging, using H α ($\lambda=6563\text{ \AA}$, $\Delta\lambda=12\text{ \AA}$) and [O III] ($\lambda=5006\text{ \AA}$, $\Delta\lambda=44\text{ \AA}$) filters was performed using a Thomson 1024 \times 1024 CCD chip at the f/3 focus of the 0.6 m Curtis Schmidt at Cerro Tololo Interamerican Observatory (CTIO) during the nights of 15–19 May 1994. The sample objects were taken from the lists of Marston *et al.* (1994) and Marston & Yocum (in preparation). It was intended that all possible shells associated with the WR stars would be identified as well as information on relative sizes and morphologies. A full listing of observations used in this paper are supplied in Table 1.

3. RESULTS ON MULTIPLE RINGS

Images of the multiple ring systems of our sample are shown in Figs. 1–5. These images allow a classification in Fig. 1(a) and (b) show new, deep images of the nebula RCW 104 in both H α and [O III] which surrounds the WR star WR75. This is the only object in our sample to show a bipolar morphology in H α . However, close inspection of Fig. 1 of Marston *et al.* (1994) shows that the nebula NGC 2359 around the star WR6 has a diffuse outer, bipolar shell, which extends to approximately 20' from the central star. The bright shell in the center is only 5' across. NGC 2359 has been shown to have multiple velocity components which may be associated with multiple ejections (Goudis *et al.* 1994). Ejected material appears to be interacting with the diffuse bipolar materials as well as a nearby molecular cloud (Marston 1991; Schneps *et al.* 1981). The shell around

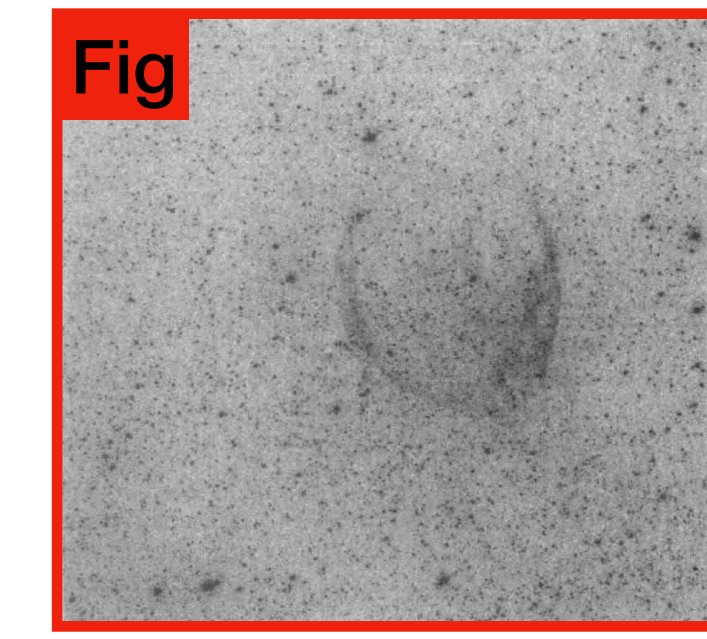
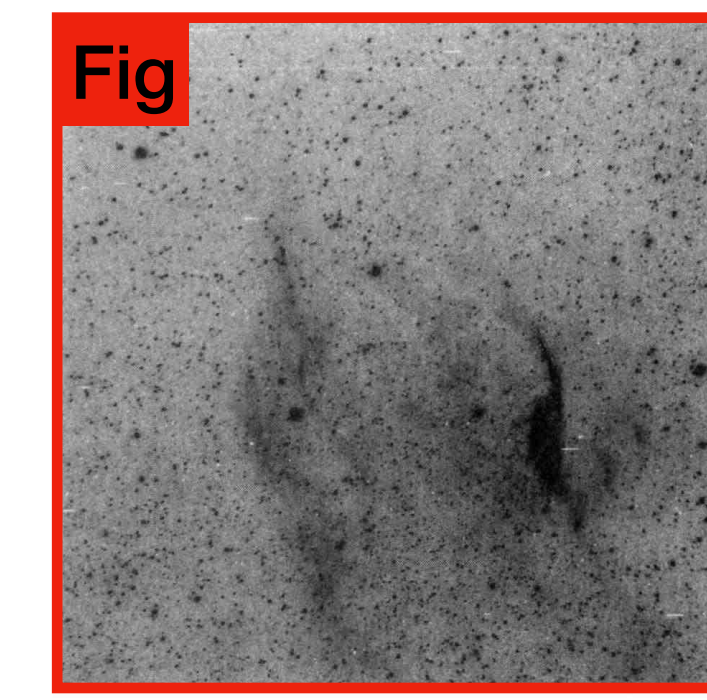


FIG. 1. (a) H α image of the filamentary, bipolar nebula RCW104 surrounding the WR star WR75. (b) Deep [O III] image of the wind-blown bubble at the center of RCW104.

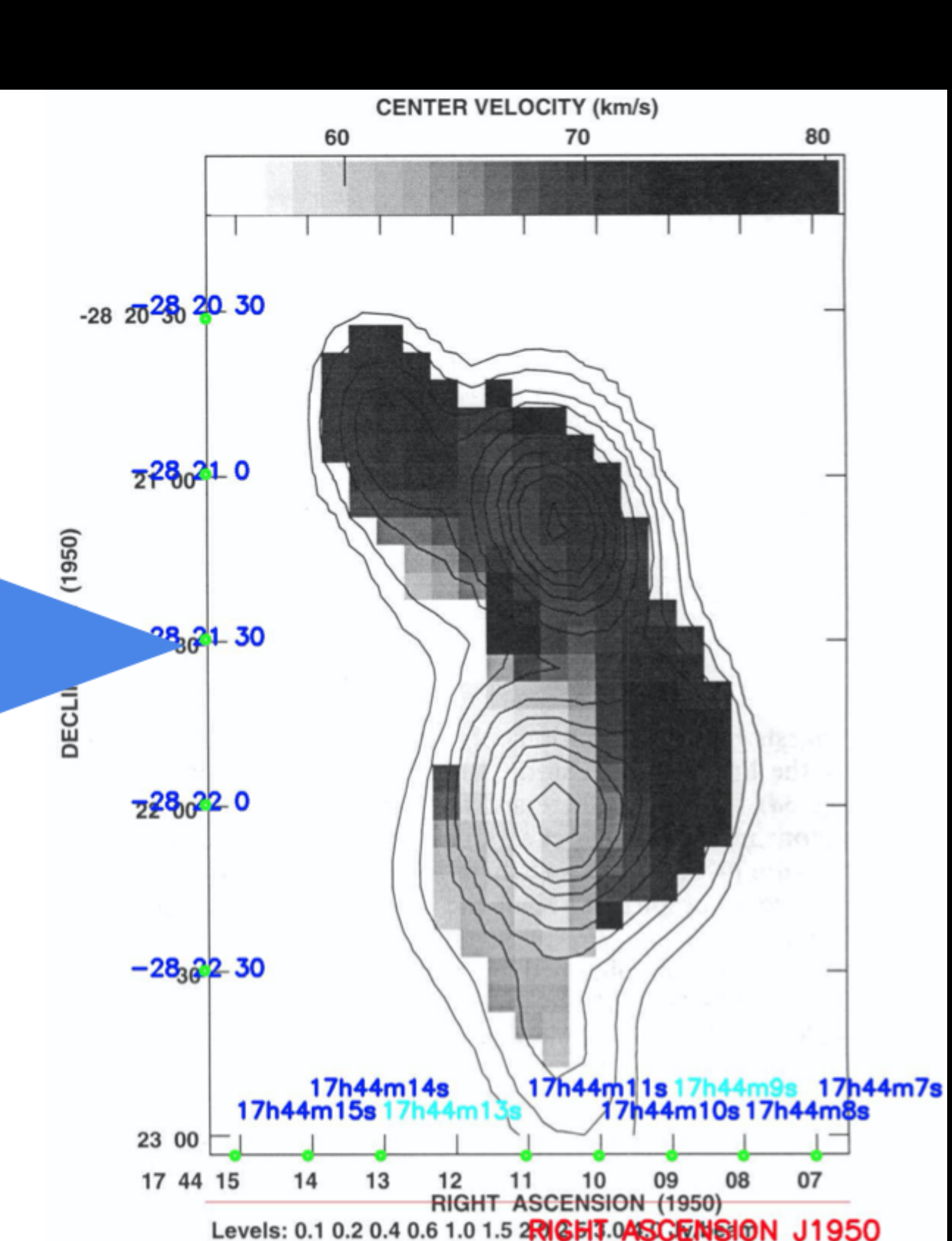
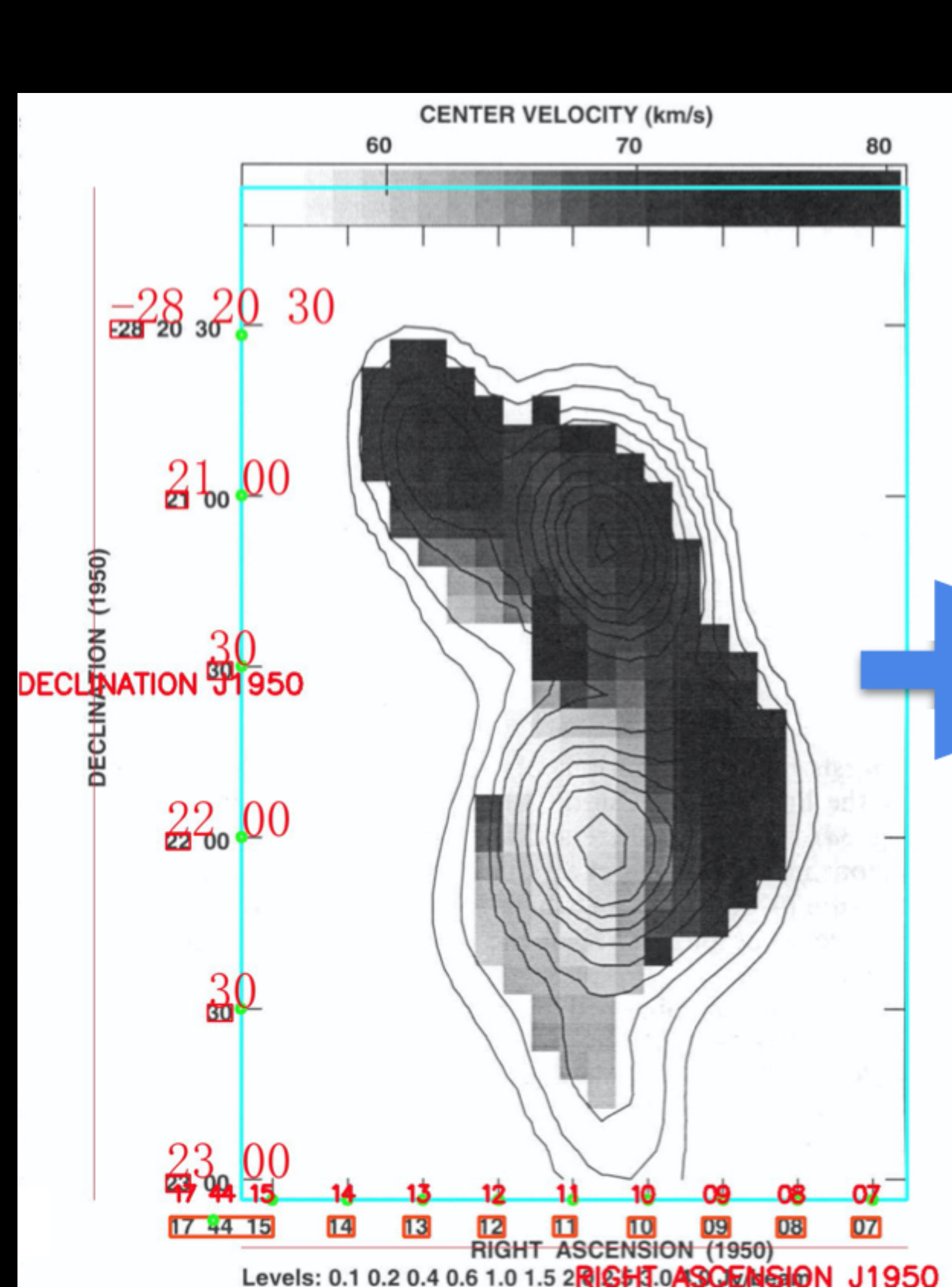
3.1 Bipolar Shells

Figures 1(a) and 1(b) show new, deep images of the nebula RCW 104 in both H α and [O III] which surrounds the WR star WR75. This is the only object in our sample to show a bipolar morphology in H α . However, close inspection of Fig. 1 of Marston *et al.* (1994) shows that the nebula NGC 2359 around the star WR6 has a diffuse outer, bipolar shell, which extends to approximately 20' from the central star. The bright shell in the center is only 5' across. NGC 2359 has been shown to have multiple velocity components which may be associated with multiple ejections (Goudis *et al.* 1994). Ejected material appears to be interacting with the diffuse bipolar materials as well as a nearby molecular cloud (Marston 1991; Schneps *et al.* 1981). The shell around

WR75 shows similar multiple components. An outer bipolar flow is outlined by strong H α filaments in the central regions while fainter lobes are observed to the north and south, extending to around 15' from the central WN6 star. An inner ring of [O III] emitting material is observed entirely within the bipolar outflow and is only 10' in diameter. The outer filaments of RCW 104 have been spectroscopically observed by Esteban *et al.* (1990), who suggest their abundances are similar to that expected from the enhanced abundances in a RSG wind. We might interpret our observations of these two bipolar nebulae as being the RSG ejecta outer filaments and relatively young WR winds interacting with the ejecta to form central cavities. The expansion of the cavities has not yet reached the edge of the RSG ejecta.

In both cases of bipolar morphology, a wind-blown (W)

1840



The Idea : How do we do this?

1840 A. R. MARSTON: RINGS AROUND WR STARS

Table 1. Multiple ring nebulae observed.					
Number	Date observed	Filter	Exposure (secs)	Figure	
WR30	16 May 1994	H α	1800	2	
WR30	15 May 1994	H α	900	3a	
WR30	19 May 1994	[OIII]	2100	3b	
WR40	HD96548	H α	1950	4a	
WR40	-	[OIII]	2100	4b	
WR75	HD14749	H α	2700	1a	
WR75	-	[OIII]	2700	1b	
WR85	HR6392B	H α	900	5	

^a uses the nomenclature of van der Hucht et al. (1981).

ejection events. This uses a similar line of argument to that proposed by Balick *et al.* (1992) for using the extended halos of planetary nebulae to distinguish the characteristics of the red giant stellar winds that existed prior to their formation.

In this paper, we provide new, deep imaging of a number of multiple rings observed around WR stars in an optical narrow-band survey made of WR stars in the southern skies. We discuss their possible implications for WR evolution and postulate what further information they may provide about the evolution of massive stars with closer investigation.

2. OBSERVATIONS

Narrow-band imaging, using H α ($\lambda=6563 \text{ \AA}$, $\Delta\lambda=12 \text{ \AA}$) and [O III] ($\lambda=5006 \text{ \AA}$, $\Delta\lambda=44 \text{ \AA}$) filters was performed using a Thomson 1024 \times 1024 CCD chip at the f/3 focus of the 0.6 m Curtis Schmidt at Cerro Tololo Interamerican Observatory (CTIO) during the nights of 15–19 May 1994. The sample objects were taken from the lists of Marston *et al.* (1994) and Marston & Yocum (in preparation). It was intended that all possible shells associated with the WR stars would be identified as well as information on relative sizes and morphologies. A full listing of observations used in this paper are supplied in Table 1.

3. RESULTS ON MULTIPLE RINGS

Images of the multiple ring systems of our sample are shown in Figs. 1–5. These images allow a classification in Fig. 1(a) and (b) show new, deep images of the nebula RCW 104 in both H α and [O III] which surrounds the WR star WR75. This is the only object in our sample to show a bipolar morphology in H α . However, close inspection of Fig. 1 of Marston *et al.* (1994) shows that the nebula NGC 2359 around the star WR6 has a diffuse outer, bipolar shell, which extends to approximately 20' from the central star. The bright shell in the center is only 5' across. NGC 2359 has been shown to have multiple velocity components which may be associated with multiple ejections (Goudis *et al.* 1994). Ejected material appears to be interacting with the diffuse bipolar materials as well as a nearby molecular cloud (Marston 1991; Schneps *et al.* 1981). The shell around

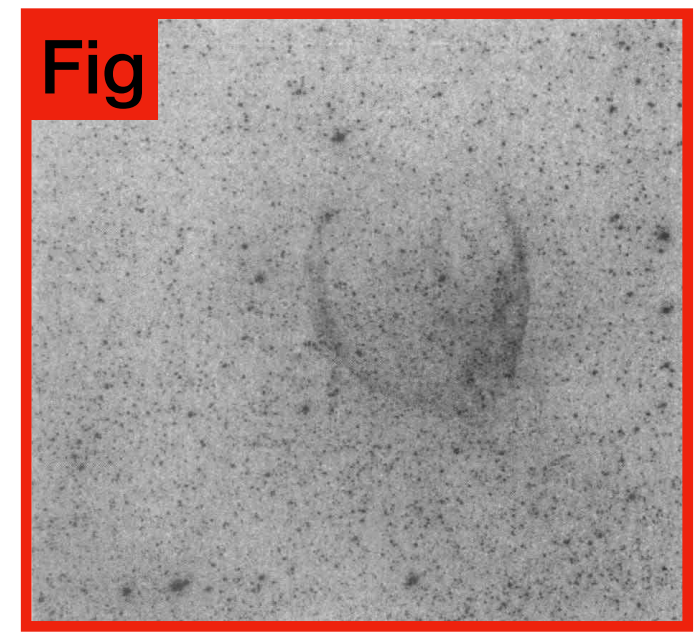
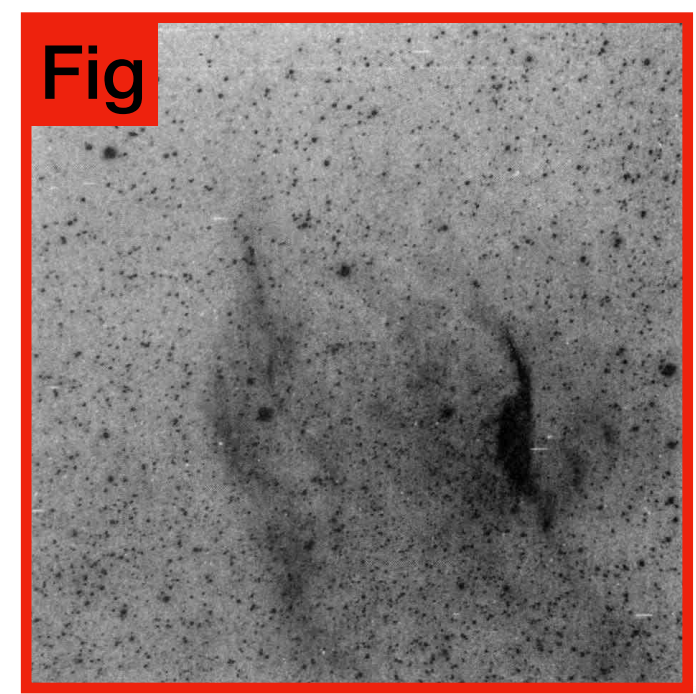


FIG. 1. (a) H α image of the filamentary, bipolar nebula RCW104 surrounding the WR star WR75. (b) Deep [O III] image of the wind-blown bubble at the center of RCW104.

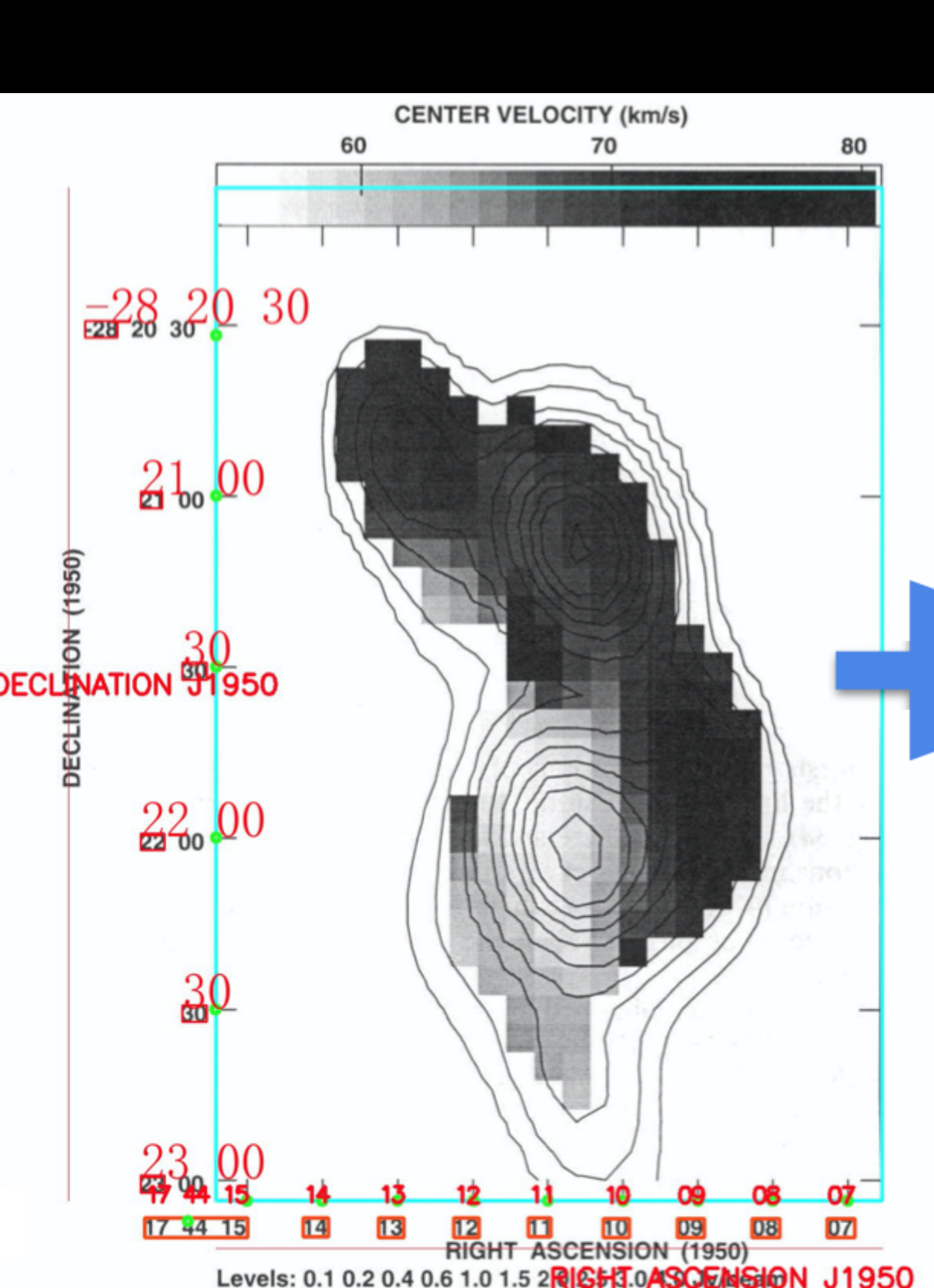
3.1 Bipolar Shells

Figures 1(a) and 1(b) show new, deep images of the nebula RCW 104 in both H α and [O III] which surrounds the WR star WR75. This is the only object in our sample to show a bipolar morphology in H α . However, close inspection of Fig. 1 of Marston *et al.* (1994) shows that the nebula NGC 2359 around the star WR6 has a diffuse outer, bipolar shell, which extends to approximately 20' from the central star. The bright shell in the center is only 5' across. NGC 2359 has been shown to have multiple velocity components which may be associated with multiple ejections (Goudis *et al.* 1994). Ejected material appears to be interacting with the diffuse bipolar materials as well as a nearby molecular cloud (Marston 1991; Schneps *et al.* 1981). The shell around

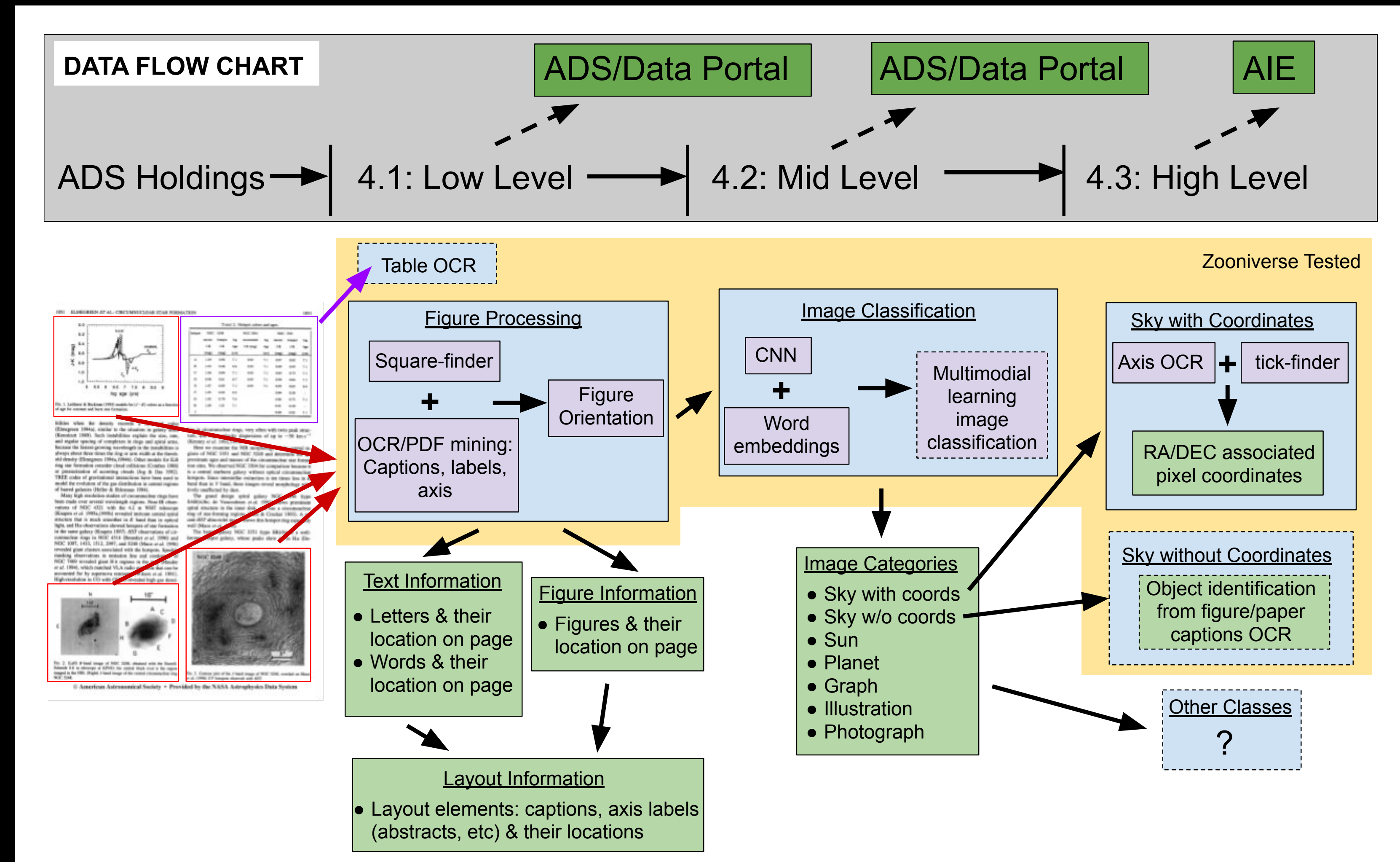
WR75 shows similar multiple components. An outer bipolar flow is outlined by strong H α filaments in the central regions while fainter lobes are observed to the north and south, extending to around 15' from the central WN6 star. An inner ring of [O III] emitting material is observed entirely within the bipolar outflow and is only 10' in diameter. The outer filaments of RCW 104 have been spectroscopically observed by Esteban *et al.* (1990), who suggest their abundances are similar to that expected from the enhanced abundances in a RSG wind. We might interpret our observations of these two bipolar nebulae as being the RSG ejecta outer filaments and relatively young WR winds interacting with the ejecta to form central cavities. The expansion of the cavities has not yet reached the edge of the RSG ejecta.

In both cases of bipolar morphology, a wind-blown (W)

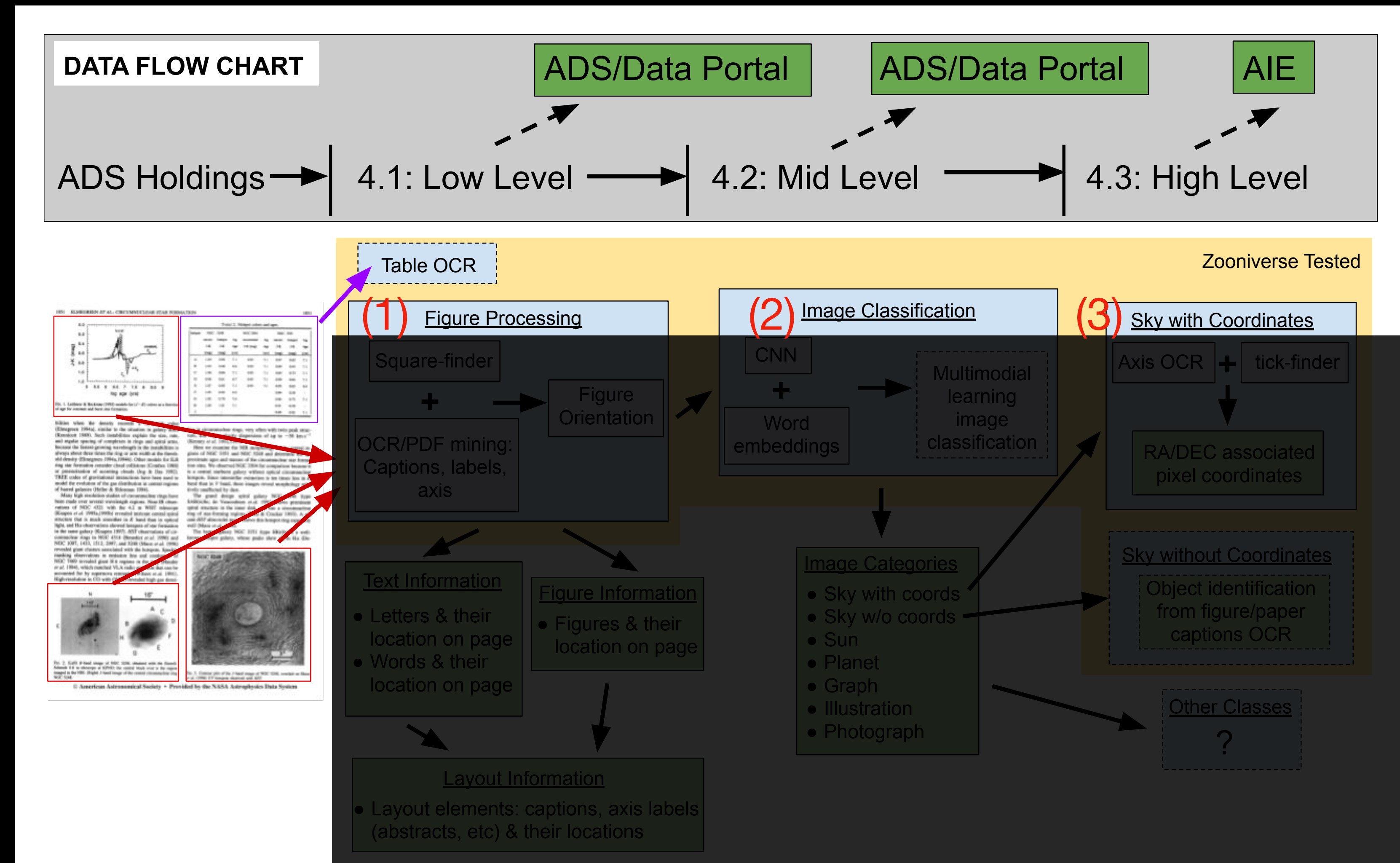
1840



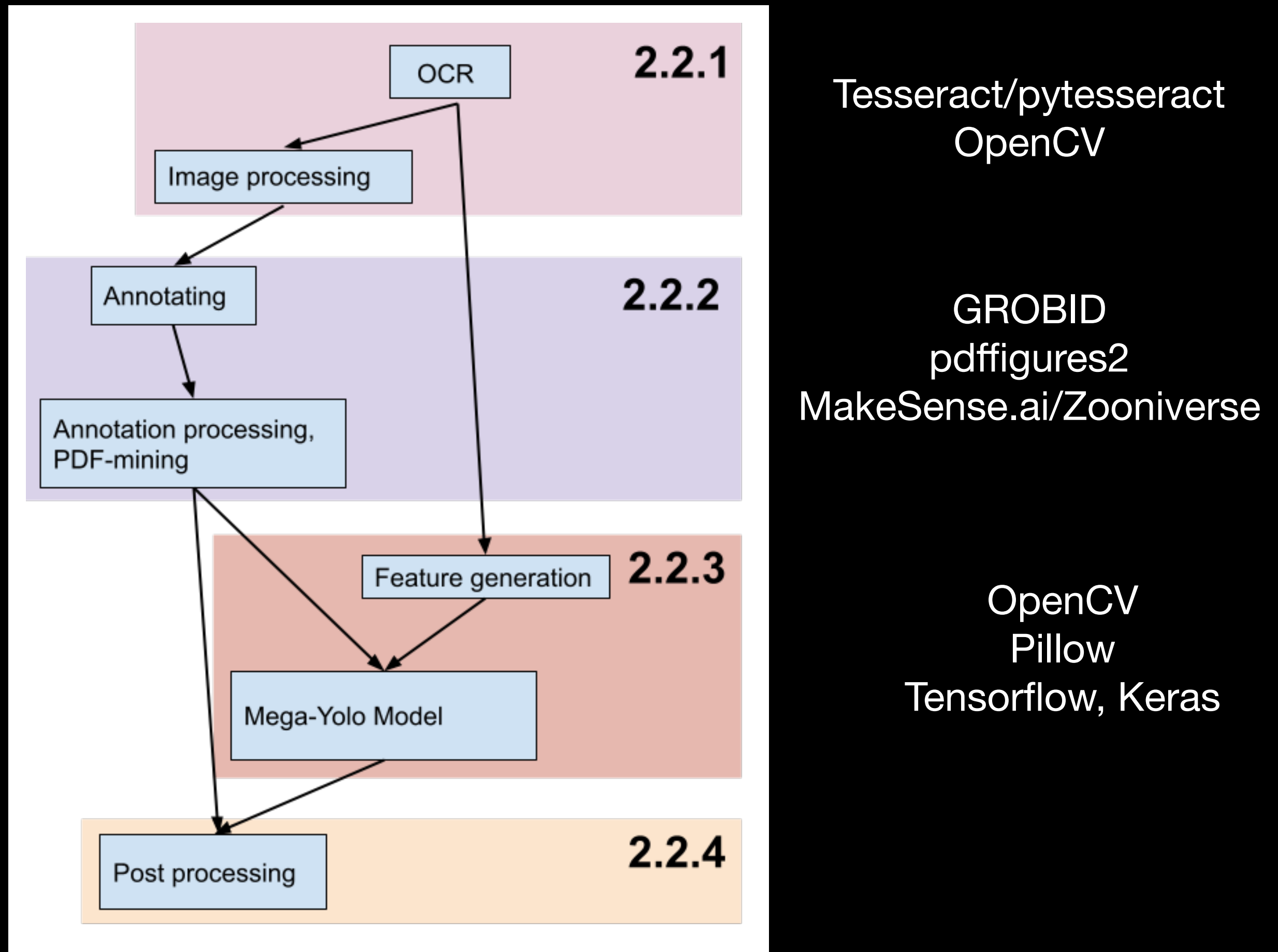
The Idea : How do we do this?



The Idea : How do we do this?



Results of our method



Tesseract/pytesseract
OpenCV

GROBID
pdffigures2
MakeSense.ai/Zooniverse

OpenCV
Pillow
Tensorflow, Keras

Naiman et al. (any day now)

Results of our method

	ScanBank No PP		ScanBank w/PP		detectron2*		detectron2*		Ours No PP		Ours w/PP	
	fig	cap	fig	cap	fig	cap [†]	fig	cap [†]	fig	cap	fig	cap
TP	69.9	29.0	69.3	52.8	72.0	46.4	81.0	80.9	58.2	23.2	85.7	86.7
FP	71.4	28.8	43.6	8.7	41.8	68.2	27.1	22.4	45.3	82.3	13.7	8.6
FN	1.7	42.8	2.5	40.7	0.6	1.6	1.2	4.9	3.1	5.1	3.5	6.0
Prec	49.5	50.2	61.4	85.9	63.3	40.5	74.9	78.3	56.2	22.0	86.2	90.9
Rec	97.6	40.4	96.5	56.5	99.2	96.6	98.5	94.3	95.0	81.9	96.1	93.6
F1	65.7	44.8	75.0	68.1	77.2	57.1	85.1	85.6	70.6	34.7	90.9	92.2

Naiman et al. (any day now)

Results of our method

fig = figure

cap = figure caption

	ScanBank No PP		ScanBank w/PP		detectron2*		detectron2*		Ours No PP		Ours w/PP	
	fig	cap	fig	cap	fig	cap [†]	fig	cap [†]	fig	cap	fig	cap
TP	69.9	29.0	69.3	52.8	72.0	46.4	81.0	80.9	58.2	23.2	85.7	86.7
FP	71.4	28.8	43.6	8.7	41.8	68.2	27.1	22.4	45.3	82.3	13.7	8.6
FN	1.7	42.8	2.5	40.7	0.6	1.6	1.2	4.9	3.1	5.1	3.5	6.0
Prec	49.5	50.2	61.4	85.9	63.3	40.5	74.9	78.3	56.2	22.0	86.2	90.9
Rec	97.6	40.4	96.5	56.5	99.2	96.6	98.5	94.3	95.0	81.9	96.1	93.6
F1	65.7	44.8	75.0	68.1	77.2	57.1	85.1	85.6	70.6	34.7	90.9	92.2

Naiman et al. (any day now)

Results of our method

fig = figure

cap = figure caption

	ScanBank		ScanBank		detectron2*		detectron2*		Ours		Ours		
	No PP		w/PP		No PP		w/PP		No PP		w/PP		
	fig	cap	fig	cap	fig	cap [†]	fig	cap [†]	fig	cap	fig	cap	
True Positive	TP	69.9	29.0	69.3	52.8	72.0	46.4	81.0	80.9	58.2	23.2	85.7	86.7
False Positive	FP	71.4	28.8	43.6	8.7	41.8	68.2	27.1	22.4	45.3	82.3	13.7	8.6
False Negative	FN	1.7	42.8	2.5	40.7	0.6	1.6	1.2	4.9	3.1	5.1	3.5	6.0
Precision	Prec	49.5	50.2	61.4	85.9	63.3	40.5	74.9	78.3	56.2	22.0	86.2	90.9
Recall	Rec	97.6	40.4	96.5	56.5	99.2	96.6	98.5	94.3	95.0	81.9	96.1	93.6
	F1	65.7	44.8	75.0	68.1	77.2	57.1	85.1	85.6	70.6	34.7	90.9	92.2

Naiman et al. (any day now)

Results of our method

fig = figure

cap = figure caption

	ScanBank		ScanBank		detectron2*		detectron2*		Ours		Ours		
	No PP		w/PP		No PP		w/PP		No PP		w/PP		
	fig	cap	fig	cap	fig	cap [†]	fig	cap [†]	fig	cap	fig	cap	
True Positive	TP	69.9	29.0	69.3	52.8	72.0	46.4	81.0	80.9	58.2	23.2	85.7	86.7
False Positive	FP	71.4	28.8	43.6	8.7	41.8	68.2	27.1	22.4	45.3	82.3	13.7	8.6
False Negative	FN	1.7	42.8	2.5	40.7	0.6	1.6	1.2	4.9	3.1	5.1	3.5	6.0
Precision	Prec	49.5	50.2	61.4	85.9	63.3	40.5	74.9	78.3	56.2	22.0	86.2	90.9
Recall	Rec	97.6	40.4	96.5	56.5	99.2	96.6	98.5	94.3	95.0	81.9	96.1	93.6
	F1	65.7	44.8	75.0	68.1	77.2	57.1	85.1	85.6	70.6	34.7	90.9	92.2

Naiman et al. (any day now)

Results of our method

fig = figure

cap = figure caption

	ScanBank		ScanBank		detectron2*		detectron2*		Ours		Ours		
	No PP	w/PP	No PP	w/PP	No PP	w/PP	No PP	w/PP	No PP	w/PP	No PP	w/PP	
	fig	cap	fig	cap	fig	cap [†]	fig	cap [†]	fig	cap	fig	cap	
True Positive	TP	69.9	29.0	69.3	52.8	72.0	46.4	81.0	80.9	58.2	23.2	85.7	86.7
False Positive	FP	71.4	28.8	43.6	8.7	41.8	68.2	27.1	22.4	45.3	82.3	13.7	8.6
False Negative	FN	1.7	42.8	2.5	40.7	0.6	1.6	1.2	4.9	3.1	5.1	3.5	6.0
Precision	Prec	49.5	50.2	61.4	85.9	63.3	40.5	74.9	78.3	56.2	22.0	86.2	90.9
Recall	Rec	97.6	40.4	96.5	56.5	99.2	96.6	98.5	94.3	95.0	81.9	96.1	93.6
	F1	65.7	44.8	75.0	68.1	77.2	57.1	85.1	85.6	70.6	34.7	90.9	92.2

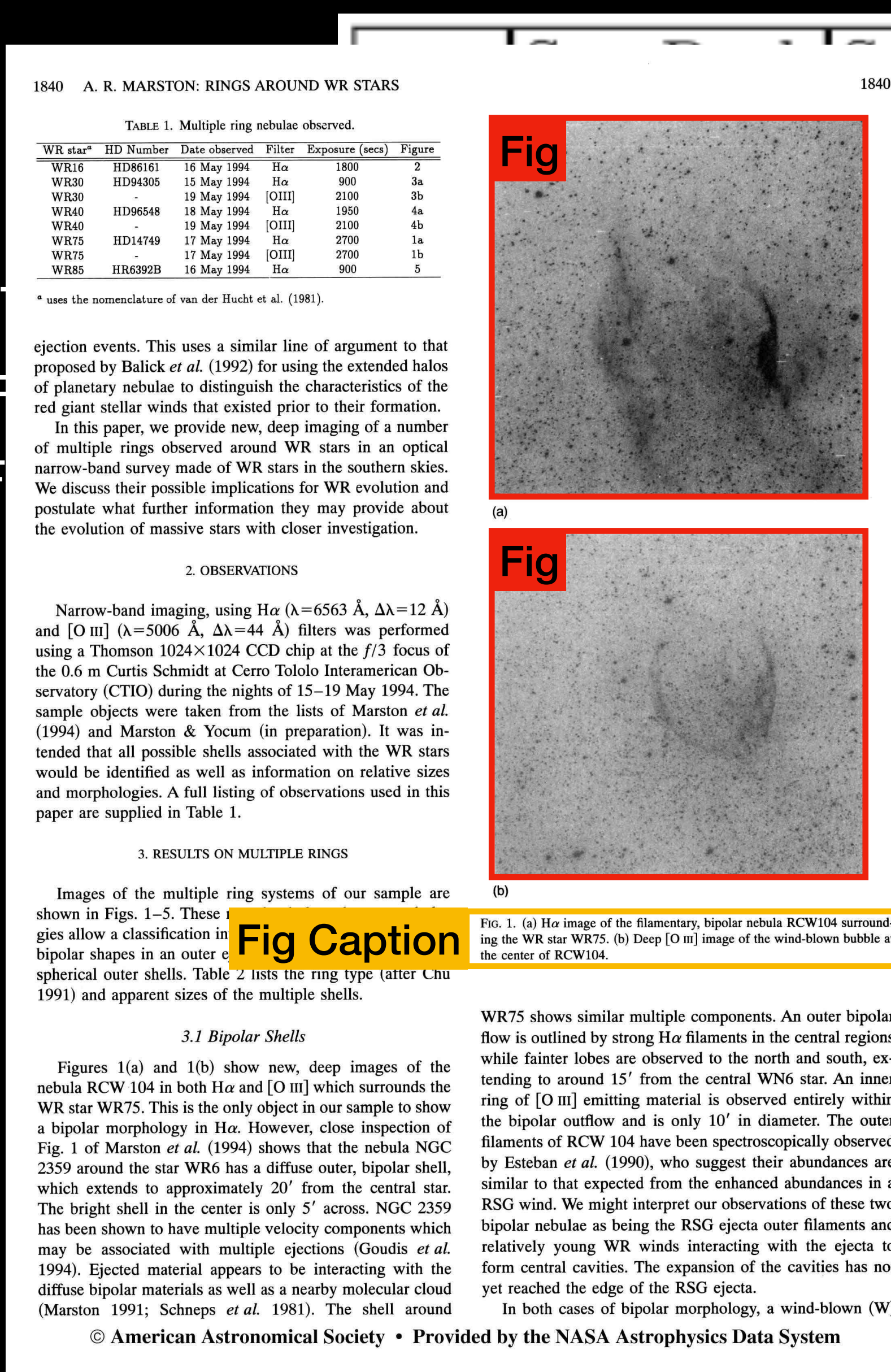
Naiman et al. (any day now)



Results of our method

fig = figure

cap = figure caption



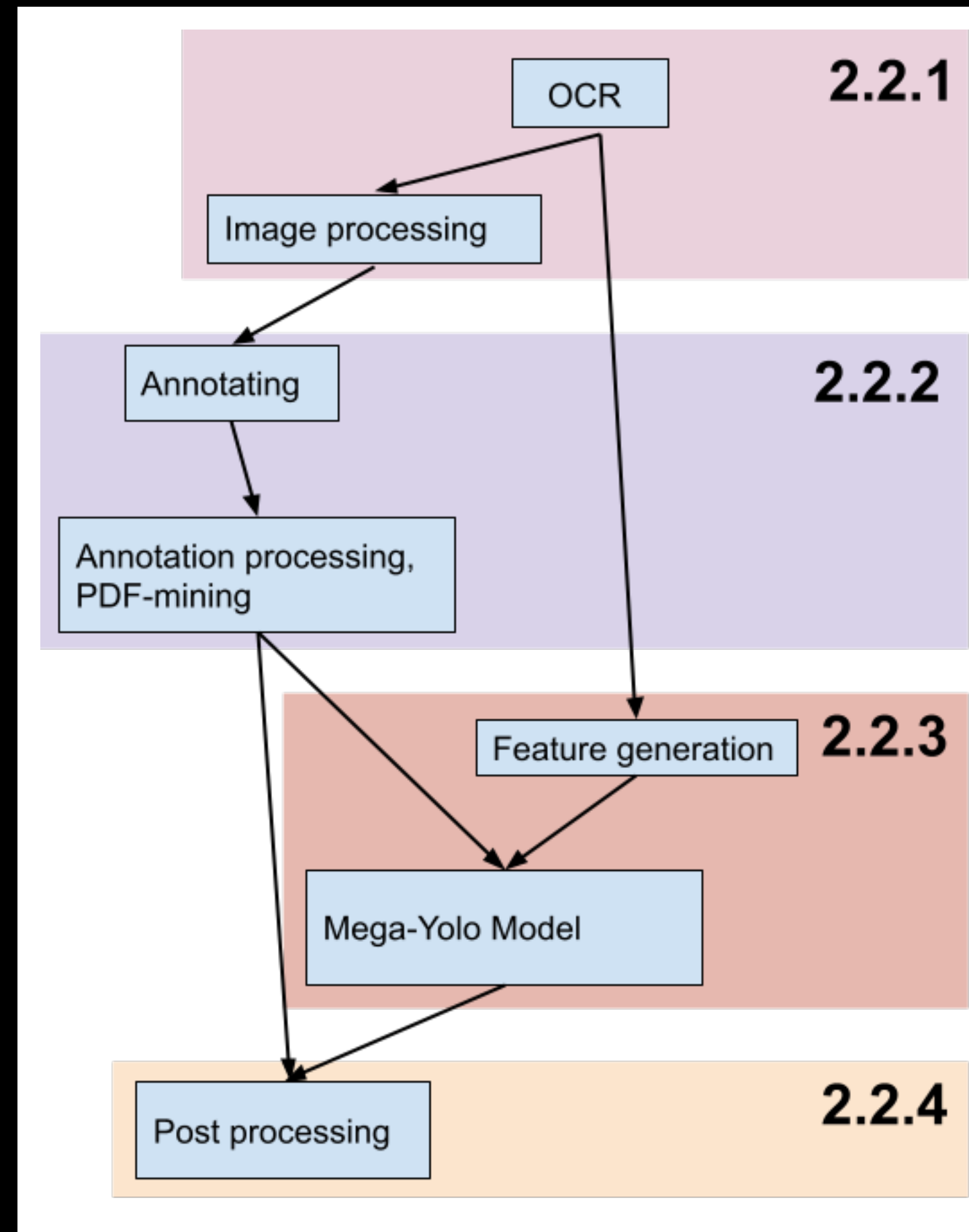
		unBank		detectron2*		detectron2*		Ours		Ours	
		v/PP ; cap	No PP ; cap	fig [†]	cap [†]	w/PP fig	w/PP cap [†]	fig	cap	fig	cap
3	52.8	72.0	46.4	81.0	80.9	58.2	23.2	85.7	86.7		
6	8.7	41.8	68.2	27.1	22.4	45.3	82.3	13.7	8.6		
5	40.7	0.6	1.6	1.2	4.9	3.1	5.1	3.5	6.0		
4	85.9	63.3	40.5	74.9	78.3	56.2	22.0	86.2	90.9		
5	56.5	99.2	96.6	98.5	94.3	95.0	81.9	96.1	93.6		
0	68.1	77.2	57.1	85.1	85.6	70.6	34.7	90.9	92.2		

Naiman et al. (any day now)

$$\text{IoU} = \frac{\text{Area of Overlap}}{\text{Area of Union}}$$

$$= 0.9$$

Results of our method



Naiman et al. (any day now)

Tesseract/pytesseract
OpenCV



Campus cluster for large batch

GROBID
pdffigures2
MakeSense.ai/Zooniverse



Zooniverse scaled for citizen
scientists
(Automatically tag machine learning
method vs citizen science)

OpenCV
Pillow
Tensorflow, Keras



AWS

Summary & Useful links

astronaiman.com

Astrophysics

- <https://www.astronaiman.com/publications.html>
- <https://www.tng-project.org/>

Data Viz

- <https://www.astronaiman.com/vizualization.html>
- <https://www.astroblend.com/> (Blender+Astro Data, hasn't been updated in a while)
- ytini.com
- <https://yt-project.org/> (scientific data analysis)
- <https://www.sidefx.com/> (Houdini)
- <https://avl.ncsa.illinois.edu/> (Advanced Visualization Lab, NCSA)
- https://uiuc-ischool-dataviz.github.io/is445_spring2022/ (this semester's Data Viz course)
- Other courses:
 - <https://www.astroblend.com/ba2016/> & <https://www.astroblend.com/ba2017/>
 - https://jnaiman.github.io/csci-p-14110_su2020/
 - https://jnaiman.github.io/csci-p-14110_su2019/

Digitization

- <https://www.astronaiman.com/digitization.html>
- <https://github.com/ReadingTimeMachine> (public with paper publishing)
- Review of document layout analysis: <https://www.mdpi.com/2076-3417/11/12/5344>

Thank you!

jnaiman@illinois.edu

